

1 Two-step obduction of the Porvenir Serpentinite: a cryptic
2 Devonian suture in SW Iberian Massif (Ossa-Morena
3 Complex)

4

5 **Rubén Díez Fernández¹, Jerónimo Matas², Ricardo Arenas³, Luis Miguel Martín-**
6 **Parra², Sonia Sánchez Martínez³, Irene Novo-Fernández³, Esther Rojo-Pérez³**

7

8 *¹Departamento de Geodinámica, Estratigrafía y Paleontología, Universidad*
9 *Complutense de Madrid, 28040 Madrid, Spain*

10 *²Instituto Geológico y Minero de España, 28003 Madrid, Spain*

11 *³Departamento de Mineralogía y Petrología, Universidad Complutense de Madrid,*
12 *28040 Madrid, Spain*

13

14 ** Corresponding author at: Departamento de Geodinámica, Estratigrafía y*
15 *Paleontología. Facultad de Geología, Universidad Complutense de Madrid, C/ José*
16 *Antonio Novais, no 2, 28040 Madrid, Spain. Tel.: +34 913944864; fax: +34 913944631*

17 *E-mail address: rudiez@ucm.es (R. Díez Fernández, corresponding author)*

18

19 **Key Points:**

- 20 • The Porvenir serpentinites represent a section of upper mantle obducted in Iberia
21 during the Variscan Orogeny

- 22 • Obduction took place in two steps, one related to Devonian
23 subduction/accretion, and another during Carboniferous out-of-sequence
24 thrusting
- 25 • The Porvenir serpentinites could be a dismembered part of a rootless Devonian
26 suture zone that may extend up to NW Iberia

27

28 **ABSTRACT**

29 The Porvenir serpentinites is a ~600 meters thick body of meta-peridotites exposed in SW
30 Iberia (Variscan Orogen). They occur as a horse within a Carboniferous, out-of-sequence
31 thrust system (Espiel thrust). This thrust juxtaposes the serpentinites and peri-Gondwanan
32 strata onto younger peri-Gondwanan strata, the serpentinites occupying an intermediate
33 position. Reconstruction of the pre-Espiel thrust structure results in a vertical
34 juxtaposition of terranes: Cambrian strata below, Porvenir serpentinites in the middle, and
35 the strata at the footwall to the Espiel thrust culminating the tectonic pile. The
36 reconstructed tectonic pile accounts for yet another major thrusting event, since a section
37 of upper mantle (Porvenir serpentinites) was sandwiched between two continental
38 tectonic slices (a suture zone *sensu lato*). The primary lower plate to the suture is now
39 overlying the upper plate due to the Espiel thrust. Lochkovian strata in the upper plate
40 and the Devonian, NE-verging folds in the lower plate suggest SW-directed accretion of
41 the lower plate during the Devonian, i.e. Laurussia-directed underthrusting for the closure
42 of a Devonian intra-Gondwana basin. Obduction of the Porvenir serpentinites was a two-
43 step process: one connected to the development of a Devonian suture zone, and another
44 related to out-of-sequence thrusting that cut the suture zone and brought upwards a
45 tectonic slice of upper mantle rocks hosted in that suture. The primary Laurussia-dipping
46 geometry inferred for this partially obducted suture zone fits the geometry, kinematics

47 and timing of the Late Devonian suture zone exposed in NW Iberia, and may represent
48 the continuation of such suture into SW Iberia.

49

50 **Keywords:** Obduction, Ophiolite, Suture Zone, Variscan Orogen, Iberian Massif

51

52 **1. INTRODUCTION**

53 Ultramafic massifs represent a common and fundamental component of ophiolite
54 complexes, and may occur at surface after obduction related to subduction zones (*Dewey,*
55 *1976; Dilek and Furnes, 2014*). The distribution of ophiolite-related ultramafic massifs
56 in an orogen may give us an idea on the number and location of suture zones (and
57 subduction zones) that contributed to orogenesis. Such an approach is valid as long as
58 there is proof that each of the exposures analyzed represents the rooting zone for a suture
59 zone. Ophiolite complexes may occur as allochthonous klippen (e.g., *Corfield et al.,*
60 *2001; Dewey, 1976*), their location being neither indicative of the actual root zone for a
61 suture, nor their current local orientation being a reflection of the primary dip-direction
62 of subduction planes. Obduction of oceanic crust and/or mantle rocks can be achieved
63 through combination of processes (e.g., *Coleman, 1981; Dewey, 1976; Godfrey et al.,*
64 *1997; Robertson, 2006; Topuz et al., 2013*). As a result, regions around suture zone
65 exposures are usually characterized by multiple deformation events, the recognition of
66 each of them being a must-do task to evaluate whether a given exposure accounts for the
67 root of a suture zone and the mechanisms involved in their obduction.

68 Suture zones are traceable, even if dismembered, due to the contrasting nature of
69 the terranes they separate, their structural position relative to major continental blocks
70 involved in the collision, or the protolith age, and timing and kinematics of accretion of
71 the ophiolites they include. But just like any other vertical juxtaposition of geological

72 elements, the upper and lower structural position of the fault-bounded domains defining
73 a suture zone can be switched by superimposed thrusting of those below onto those above
74 (e.g., out-of-sequence thrusts). Such a consideration impacts dramatically on the
75 reconstruction of major tectonic processes in mountain belts, as upper and lower plates
76 relative to subduction zones may be observed in the opposite position they had during the
77 suturing process (Fig. 1).

78 With the aforementioned ideas in mind, we present a structural analysis of a region
79 around a several hundred meters thick tectonic slice of meta-peridotites (Porvenir
80 serpentinites) that is exposed in SW Iberia. Reconstruction of the several phases of
81 deformation that affected the meta-peridotites and the rocks resting on top and below
82 them demonstrates that the obduction of the ultramafic massif was achieved through a
83 two-step process during the Variscan Orogeny. In the Late Devonian, the meta-peridotites
84 were part of a suture zone, in which upper mantle rocks ended up bounded by two tectonic
85 slices of peri-Gondwanan continental crust. Then, during the Carboniferous, (steeper)
86 out-of-sequence thrusts cut across the former suture zone, and transported onto its upper
87 plate a dismembered section of the suture zone (meta-peridotites) along with the lower
88 plate. A short discussion frames this sequence of events in the geological evolution of the
89 region and analyzes the impact of our two-step obduction model for the evolution of the
90 Variscan Orogen in Iberia.

91

92 **2. GEOLOGICAL SETTING**

93 The pre-Mesozoic structure of the Iberian Massif resulted from the progressive
94 collision between Gondwana, Laurussia and their peripheral terranes after the closure of
95 the Rheic Ocean (Variscan Orogen; *Díez Fernández et al.*, 2016; *Martínez Catalán et al.*,
96 2009; *Matte*, 2001; *Ribeiro et al.*, 2007; *Simancas et al.*, 2013). The origin of the

97 peripheral terranes are, in most cases, somewhat related to the opening, widening and
98 eventual closure of the Rheic Ocean (*Albert et al., 2015; Arenas and Sánchez Martínez,*
99 *2015; Chichorro et al., 2008; Díez Fernández et al., 2010; Linnemann et al., 2008;*
100 *Sánchez-García et al., 2003*). A number of peri-continental, Gondwana-derived terranes
101 (Ediacaran – Ordovician arc-related terranes) are found as tectonic slices on top of
102 inboard sections of the platform of mainland Gondwana, both in the NW section (*Arenas*
103 *et al., 1986; Martínez Catalán et al., 2007; Ribeiro et al., 1990*) and SW section (*Araújo*
104 *et al., 2005; Azor et al., 1994; Díez Fernández et al., 2017*) of the Iberian Massif (Fig. 2).

105 Whether or not the Gondwanan terranes of Iberia were part of a single, currently
106 dismembered, peri-Gondwanan micro-continent (*Díez Fernández and Arenas, 2015*), or
107 individual terranes transferred to such structural position by means of different processes
108 across the margin of Gondwana (*Martínez Catalán, 1990; Ribeiro et al., 2007; Simancas*
109 *et al., 2013*), relies on the existence of a common major thrust (or thrust system) able to
110 explain their emplacement. According to *Díez Fernández and Arenas (2015)*, the suturing
111 of an intra-Gondwana Devonian basin, carried out in the context of Laurussia-directed
112 subduction-accretion and underthrusting, can explain the uppermost structural position
113 this collection of peri-Gondwanan terranes share today. This way, the exposures of this
114 putative suture zone should contain lithological assemblages that experienced high-P
115 metamorphism roughly at the same time, and be accompanied by ophiolitic assemblages
116 that were located in a Devonian basin before obduction. These two requisites are fairly
117 met by the lithological assemblages that have been proposed as tracers for this single
118 intra-Gondwana suture zone across the Iberian Massif (*Abati et al., 2018; Díez Fernández*
119 *and Arenas, 2015; Díez Fernández et al., 2016, 2017*). There is also good similarity and
120 geochemical and isotopic affinities between the sedimentary series involved in the suture

121 zone of the Devonian basin that are now observed hundreds of kilometers away from each
122 other in NW and SW Iberia (*Díez Fernández et al., 2017*).

123 Another angle to test the verisimilitude of the model would be to prove that the
124 primary regional dip of the major thrust that emplaced the suture zone, and therefore the
125 peri-Gondwanan terranes to their current upper structural position, is the same across the
126 Iberian Massif (in paleogeographic terms). Subduction polarity for the closure of the
127 intra-Gondwana Devonian basin and subsequent underthrusting is well-constrained in
128 NW Iberia. Structural and tectonometamorphic analyses carried out in the Basal
129 Allochthonous Units of NW Iberia strongly support Laurussia-directed subduction and
130 underthrusting (W-dipping in present-day coordinates; *Díez Fernández et al., 2011, 2012*;
131 *Martínez Catalán et al., 1996*). Should this major thrusting event affect rocks now
132 exposed in other parts of the Iberian Massif (e.g., SW Iberia), the regional dip of thrust
133 planes for those events (subduction + underthrusting) should be compatible. So far
134 subduction polarity for the Central Unit, which is considered a member of the single intra-
135 Gondwana suture zone in SW Iberia by *Díez Fernández and Arenas (2015)* (Fig. 2), is
136 assumed to be towards Gondwana (NE-dipping in present-day coordinates; *Azor et al.,*
137 *1994; Pereira et al., 2010*), i.e., opposite that inferred for equivalent rocks in NW Iberia.

138 We have selected a study area located in the Obejo-Valsequillo Domain (Ossa-
139 Morena Complex of SW Iberia; Figs. 2 and 3), a section of the Iberian Massif dominated
140 by tectonic slices with continental crust affinity that also contains minor and dispersed
141 units with oceanic crust or upper mantle affinity. From a paleogeographic point of view,
142 the sedimentary sequences of this domain are widely accepted as deposited in basins
143 connected to Gondwana (*Robardet and Gutiérrez Marco, 2004; Talavera et al., 2015*),
144 whose age range from Ediacaran up to Carboniferous (see revision by *Martínez Poyatos,*
145 *2002; Matas et al., 2015a*). Although Cadomian (Ediacaran-Cambrian) deformation has

146 been inferred for the oldest rocks of this domain (e.g., *Blatrix and Burg, 1981; Dallmeyer*
147 *and Quesada, 1992; Eguíluz et al., 2000; Llopis et al., 1970; Martínez Poyatos et al.,*
148 *2001*), its current regional architecture is largely controlled by structures formed during
149 the late Paleozoic, in the course of the Variscan Orogeny (*Apalategui and Pérez-Lorente,*
150 *1983; Azor et al., 1994; Martínez Poyatos et al., 1995b, 1998a*).

151 In the Obejo-Valsequillo Domain, Ediacaran through to Devonian and
152 Carboniferous lithostratigraphic series are affected by folds, faults and ductile shear
153 zones. A NE-verging train of overturned to recumbent folds has been identified as the
154 first Variscan (Devonian) deformation in this domain (*Azor et al., 1994; Martínez Poyatos*
155 *et al., 1995a, 1995b, 1998a*). These folds only affect pre-Late Devonian rocks and were
156 generated under low- to medium-grade metamorphic conditions (*López Munguira et al.,*
157 *1991; Martínez Poyatos, 2002*). A numerous set of NE-directed thrusts is a contributor to
158 the Variscan structure of the Obejo-Valsequillo Domain (Fig. 3). These thrusts cut across
159 the aforementioned Devonian folds and are in close relation to the development and
160 evolution of (syn-orogenic) Carboniferous sedimentary basins, which in some cases post-
161 date and in other cases are affected by Variscan structures (*Martínez Poyatos et al.,*
162 *1998b; Wagner, 2004*). Among these thrusts, the Espiel thrust stands out as being
163 responsible for the duplication of the Precambrian and Paleozoic lithostratigraphy across
164 this domain and for the overriding of metamorphic onto non-metamorphic rocks
165 (*Apalategui and Pérez-Lorente, 1983; Martínez Poyatos et al., 1995b, 1998a; Matas et*
166 *al., 2015a*).

167 The boundaries of the Obejo-Valsequillo Domain are late Variscan shear zones.
168 The Puente Génave – Castelo de Vide detachment (*Martín Parra et al., 2006*) marks the
169 contact with the Central Iberian Zone, located to the North (Fig. 2; *Díez Fernández and*
170 *Arenas, 2015*). The Matachel normal fault (*Azor et al., 1994*), along with the Ojuelos-

171 Coronada igneous complex (*Delgado Quesada, 1971*), can be taken as the southern
172 boundary of the Obejo-Valsequillo Domain (Fig. 3).

173 South of the Obejo-Valsequillo Domain, the Central Unit represents a Variscan
174 suture zone (*Azor, 1994*). High-P metamorphism in this unit (*Abalos et al., 1991b; Mata
175 and Munhá, 1986*) has been dated at Late Devonian (*Abati et al., 2018*), whereas post-
176 eclogite metamorphic evolution related to its exhumation is constrained to Late Devonian
177 through to Carboniferous (*Dallmeyer and Quesada, 1992; Pereira et al., 2010*). The
178 Central Unit consists of mid- to high-grade gneisses and minor amphibolites (including
179 retroeclogites) that is thrust onto an ensemble of low- to mid-grade metamorphic rocks
180 referred to as the Albarrana Domain (Fig. 2), which is considered the relative autochthon
181 to the Central Unit suture (*Azor, 1994; Azor et al., 1994; Simancas et al., 2001*). Many of
182 the thrusts and extensional faults of the region show a component of left-lateral oblique-
183 slip, their functioning being attributed to a Variscan, oblique plate boundary system (e.g.,
184 *Pérez-Cáceres et al., 2016*).

185 The study area is located well inside the Obejo-Valsequillo Domain (Fig. 3). It
186 includes an exceptional exposure of the rocks and structures that are non-affected (post-
187 date), are affected by, or are affecting the Espiel thrust (Fig. 4a), making it a good site to
188 constrain the tectonic record of this major fault. Given that the Espiel thrust transported
189 Middle-Late Devonian folds in its hanging-wall (*Simancas et al., 2001*), a reconstruction
190 of the deformation by this fault would provide clues to the geometry of Middle-Late
191 Devonian structures. First descriptions of the Espiel thrust reported the existence of a
192 body (several hundred meters thick) of serpentinites (meta-peridotites) along its trace
193 (*Apalategui and Pérez-Lorente, 1983*). This occurrence represents a first-order anomaly
194 in SW Iberia, as it represents a tectonic slice of upper mantle bounded by continental crust
195 above and below, thus reproducing the essentials for an exhumed suture zone.

196

197 **3. LITHOSTRATIGRAPHY OF THE STUDY AREA**

198 The bedrock geology of the study area is defined by five groups of rocks (Fig. 4a).
199 Two of them correspond to the hanging wall (Cambrian metasedimentary rocks; low-
200 grade metamorphism) and footwall (Cambrian-Ordovician and Silurian-Devonian
201 metasedimentary and metaigneous rocks; very low-grade metamorphism or non-
202 metamorphosed) of the Espiel thrust. A third group occurs in an intermediate position
203 within the Espiel thrust, and features a complex fault zone separating the fault's hanging
204 wall and footwall. It includes lens-shaped fault-bounded domains, in which the most
205 salient, internally coherent domain is made of meta-peridotites (Porvenir serpentinites).
206 The rest of the fault-bounded domains are dispersed along the fault trace and include
207 variably deformed meta-igneous (granitoid) rocks and phyllonites after Carboniferous
208 metasedimentary rocks. Each outcrop of the fault zone is made of the same, yet variably
209 strained, lithology, and the set of fault-bounded domains do not share a matrix of any sort
210 (either serpentinitic or sedimentary), i.e. they do not show block-in-matrix structure. A
211 fourth group is represented by Carboniferous (Variscan) syn-orogenic sedimentary rocks,
212 whereas the fifth group consists of a discordant, non-deformed Cenozoic sedimentary
213 cover.

214

215 **3.1. Hanging wall to the Espiel thrust**

216 Three main concordant members can be distinguished in the upper part of the
217 hanging wall to the Espiel thrust. Local way-up criteria such as cross-bedding and normal
218 graded bedding, together with structural criteria (see section 4.1), were used to solve
219 stratigraphical polarity.

220 The lower (older) member consists of thin-bedded, grey to dark-grey phyllites
221 alternating with white to light-grey metasandstones (greywackes). The thickness for both
222 ranges between few millimeters up to several centimeters, whereas a minimum thickness
223 of 2.5 Km can be inferred for the whole member. Quartzite beds observed towards the
224 lower part of the member could be part of a quartzite-rich horizon that extends for several
225 Km over the study area.

226 The intermediate member includes phyllites (similar to those of the lower
227 member) and more abundant and thicker layers of metasandstones (greywackes) and
228 quartzites. Quartzites do not define a mappable layer within this unit, as they occur at any
229 level in this succession. This member is ~1 Km thick and represents a transition towards
230 the upper member.

231 The upper member consists of quartzites and feldspar-rich metasandstones that
232 alternates with light-grey to pinkish phyllites. Metasandstone beds range between several
233 decimeters and several meters in thickness, the thickest ones being at the top of the series.
234 Minimum thickness for this member is at ~150 m.

235 This succession, especially the two lower members, are lithologically identical to
236 the Azuaga Formation (*Delgado Quesada, 1971*), also referred to as the Villares
237 Formation by *Liñán (1978)*. This idea has been put forward before (e.g., *Apalategui et*
238 *al., 1985; Matas et al., 2015a*). The age of the Azuaga Fm. (based on fossil content) is
239 Early-Middle Cambrian (*Azor, 1994; Liñán, 1978; Liñán and Quesada, 1990; Jensen et*
240 *al., 2004*), so a similar age is assumed for the series described here.

241

242 **3.2. Intermediate fault-bounded domains of the Espiel thrust**

243 *3.2.1. Porvenir serpentinites*

244 This unit consists of ~600 meters of serpentinized ultramafic rocks that crops out
245 NE of the El Porvenir village (Fig. 4a). The maximum thickness of this unit has been
246 calculated assuming an average dip of 40° for the foliation. Previous works mentioned
247 the existence of lenses metabasites and gneisses within this unit (*Apalategui et al.*, 1982),
248 but recent fieldwork has not confirmed those observations yet. Those lenses were located
249 on top and below the main body of serpentinites, thus suggesting they could be part of
250 different tectonic slices. Most of the serpentinites in this body show massive structure,
251 although foliated serpentinites occur as variably thick (cm to m) layers separating beds of
252 massive serpentinites (Fig. 5a). The serpentinites are green to yellow-brown-green, and
253 include serpentine minerals, pseudomorphs after olivine and minor pyroxene, dark red
254 spinel, magnetite, phlogopite, chlorite, sericite, and talc (Fig. 5b) (*Apalategui et al.*,
255 1982). Olivine pseudomorphs represent more than 80% of the rock volume in all the
256 samples collected. The serpentinized mineral assemblage points to dunite as the most
257 likely protolith for the Porvenir serpentinites. Dunite is one major constituent of Earth's
258 upper mantle, and is typically found in the lower sections of ophiolitic complexes.

259

260 3.2.2. *Undifferentiated metaigneous rocks*

261 A series of variably deformed and recrystallized igneous rocks occurs along the
262 Espiel thrust. In most cases they show heterogeneous mylonitic fabric. These metafelsic
263 rocks are dominantly made of cm-scale grains of quartz, K-feldspar and plagioclase
264 surrounded by a matrix of fine-grained quartz, feldspar and mica (mostly biotite) that are
265 compatible with a primary porphyritic texture for their plutonic protoliths. The absence
266 of individual lens-shaped, highly stretched layers rich in feldspar or quartz in these rocks
267 suggest that most of the mylonitic foliation developed at the expense of the ground mass
268 of porphyritic granitoids. Quartz and feldspar porphyroclasts are partially recrystallized,

269 the former phenocrysts being now an ensemble of quartz and feldspar subgrains and
270 newly crystallized grains of quartz, feldspar, plagioclase, mica, sericite and opaques. The
271 fine-grained matrix is made of a statistically oriented mass of those same minerals,
272 slightly richer in quartz, mica and sericite. No age constraints are available for their
273 protoliths. Straightforward recognition of lithostratigraphic affinities with other units of
274 the region is not possible due to the limited and poor-quality of the outcrops and by
275 intense strain.

276 Metavolcanics are another type of metaigneous rock found in the fault zone,
277 including acid volcanic tuffs and volcanoclastic sandstones with fragments of limolite or
278 quartzite (*Apalategui et al.*, 1982).

279

280 3.2.3. Gneisses

281 Descriptions of the fault zone of the Espiel thrust suggested the presence of
282 gneisses, amphibolites, mylonites and phyllonites equivalent to those that occur in the
283 Central Unit (*Apalategui and Pérez-Lorente*, 1983). We were only able to find an outcrop
284 of mylonitic gneisses, which certainly reminds rocks of the Central Unit. The gneisses
285 are different and accumulate more strain than any other type of rock in the hanging wall
286 or footwall to the Espiel thrust, and must be considered exotic within the fault zone like,
287 for instance, the Porvenir serpentinites.

288 The mylonitic gneisses show a compositional banding defined by quartz-
289 feldspathic-rich layers, which contain minor mica, alternating with layers richer in mica,
290 and layers made exclusively of quartz and mica. Individual grains of quartz, feldspar,
291 plagioclase, and mica (mostly biotite) parallel the main foliation, as do lens-shaped
292 aggregates of biotite, opaque minerals, minor white mica and rare garnet.

293

294 **3.3. Footwall to the Espiel thrust**

295 *3.3.1. Cambrian - Ordovician series*

296 The older metasedimentary succession is terrigenous. The lower part of the series
297 includes meta-arkoses, quartzites, metaconglomerates and some felsic metavolcanics,
298 while the upper part contains quartzites, slates and minor metalimestones. The lower part
299 of this series has been considered as Cambrian-Ordovician (*Matas et al.*, 2015a), whereas
300 the upper part has been correlated with the Armorican quartzite on the basis of lithological
301 composition and fossil content (*cruziana* and *skolithos*, among other), which indicates a
302 Paleozoic age, most likely Ordovician (*Gutiérrez-Marco et al.*, 2002).

303

304 *3.3.2. Silurian-Devonian series*

305 The structurally lower metasedimentary succession that can be recognized in the
306 study area consists of Fe-rich quartzites, metasandstones, brown and black slates,
307 metavolcanics, and minor dark-grey, bioclastic limestones. The slates alternate with the
308 metasandstones and quartzites at the millimeter- to centimeter-scale, but the latter can
309 reach up to several meters in thickness and tens of meters in lateral continuity. The
310 distribution of these lithologies does not follow an homogeneous pattern, but the
311 limestones are more common towards the lower part of the succession. The lowermost
312 limestones contain Ludlowian fossils, whereas the rest contain Lochkovian fauna
313 (*Apalategui et al.*, 1982), indicating that the Silurian-Devonian transition occur within
314 this succession and a lack of early Silurian and mid-late Devonian strata. The nature of
315 the basal contact of this series has not been observed.

316

317 **3.4. Carboniferous syn-orogenic series**

318 The age of the youngest Devonian and the oldest Carboniferous series in the
319 region is younger than the (Devonian) onset of Variscan deformation in SW Iberia, and
320 the youngest Carboniferous series is affected by Variscan deformation. For these reasons,
321 the Late Devonian and Carboniferous sedimentary rocks are considered as syn-orogenic
322 (e.g., *Wagner, 2004*). Late Devonian rocks are not exposed in the study area. The
323 Carboniferous series are divided in three groups according to their age and facies
324 (*Martínez Poyatos, 2002*).

325

326 3.4.1. C1: Tournaisian – Upper Viséan to Serpukhovian (*Culm facies*)

327 This series consists of an alternation of slates and metagreywackes at the cm- to
328 dm-scale, and minor metaconglomerates, marbles, and metavolcanics (whole rock, K/Ar
329 crystallization ages of 348 ± 17 Ma and 334 ± 17 Ma; *Bellon et al., 1979*). Commonly
330 referred to as *Culm facies*, similar rocks of this type are intruded by igneous rocks dated
331 at 332 ± 17 Ma (whole rock, K/Ar; *Bellon et al., 1979*) and ~ 307 Ma (U-Pb in zircon,
332 single grains; *Carracedo et al., 2009*). Marine fossils yielded Upper Tournaisian – Upper
333 Viséan ages (e.g., *Garrote and Broutin, 1979*), Lower through to Upper Tournaisian ages,
334 and Lower Tournaisian up to Serpukhovian ages (*Matas et al., 2015a*), depending on the
335 section. Deposition of the lower part of this series has been interpreted as related to an
336 extensional event, whereas the upper part has been related to crustal shortening
337 (*Armendariz et al., 2008; Martínez Poyatos, 2002*).

338

339 3.4.2. C2: Upper Viséan – Serpukhovian (*Granja de Torrehermosa Beds*)

340 This series includes sandstones, conglomerates, lutites, limestones, some rhyolites
341 and minor coal beds. Limestone beds occur in an intermediate level of the series, while
342 coal is found towards the top. Pebbles of rocks from the *Culm facies* were found in some

343 conglomerates (*Pérez Lorente, 1979*). Marine and continental fossils collected in this
344 series constrain the age to Upper Viséan – Serpukhovian (*Apalategui et al., 1985; Mamet*
345 *and Martínez, 1981; Ortuño, 1971*).

346

347 3.4.3. C3: Bashkirian – Moscovian (*Peñarroya Beds*)

348 The base of this succession includes a 50m to >400m thick layer of conglomerates
349 that alternates with minor sandstones and lutites, and is overlain by sandstones, silts, and
350 lutites that intercalate coal beds. Conglomerate pebbles include black, red, and white
351 quartzites, slates, other conglomerates and sandstones, and limestones from the Granja de
352 Torrehermosa Beds (*Andreis and Wagner, 1983*). Previous authors (e.g., *Andreis and*
353 *Wagner, 1983; Pérez Lorente, 1979*) suggested a provenance from the North (present-day
354 coordinates). However, several observations of SW-dipping imbricated clasts in the basal
355 conglomerates suggest NE-directed flow, i.e., a source area probably located to the SW.

356

357 4. PHASES OF DEFORMATION

358 Variscan deformation in the study area can be grouped in three major phases. The
359 first phase (D_1) produced NE-verging overturned folds and an associated axial planar
360 foliation (S_1). The second one (D_2) corresponds to the development of the NE-directed
361 Espiel thrust and related local fabrics (S_2). The third one (D_3) produced local foliation
362 (S_3), the re-folding of D_1 folds, the folding of the Espiel thrust, and a new generation of
363 NE-directed thrusts.

364

365 4.1. NE-verging overturned folds (D_1)

366 The rocks of the hanging wall and, to a minor extent, the footwall to the Espiel
367 thrust show a penetrative foliation (S_1 ; Figure 5c). S_1 (for metapelites) in the hanging

368 wall is defined by recrystallized quartz, plagioclase, chlorite, white mica, opaques, and
369 minor biotite and garnet (low-grade metamorphism), whereas in the footwall the main
370 foliation is marked by reoriented sedimentary clasts of quartz, feldspar, plagioclase and
371 mica and the preferred orientation of newly-formed chlorite and sericite (very low-grade
372 metamorphism). S_1 ranges between slaty and phyllitic, the more granular facies showing
373 spaced and rough cleavage.

374 An intersection lineation (Li_1) varies across the study area. The cleavage-bedding
375 relationship, together with local way-up criteria, were used to identify upright and
376 overturned limbs of major D_1 folds, for which S_1 maintains an axial planar geometry.
377 Two fold closures of the same major syncline (Espartal syncline) are observed. That
378 syncline dominates the internal structure of the hanging wall to the Espiel thrust, its
379 upright limb occupying the northern exposures and the overturned limb the southern ones
380 (Fig. 4c).

381 Regional dip-direction for both limbs (S_0) changes, but a SW-dipping direction is
382 common (Fig. 6a). S_1 shows dominant SW-dipping geometry (Fig. 6b) although it dips
383 to the NE in some parts. Li_1 trends NW-SE and is gently-plunging, plunging NW and SW
384 (Fig. 6c), explaining two consecutive fold closures of the Espartal syncline in a NW-SE
385 direction (Fig. 4a).

386 The maximum age for D_1 is constrained by the age of the youngest series affected
387 by S_1 , the Early Devonian (Lochkovian to Emsian) rocks of the footwall to the Espiel
388 thrust (*Matas et al.*, 2015a). The minimum age is defined by the Late Devonian
389 (Famenian) to Early Carboniferous (Tournaisian) rocks that are affected by the Espiel
390 thrust (*Matas et al.*, 2015a), which cuts across D_1 folds (see section 4.2).

391

392 **4.2. The Espiel thrust (D_2)**

393 The juxtaposition of Cambrian onto Cambrian-Ordovician and Silurian-Devonian
394 rocks resulted from the second phase of deformation. The contact between the upper
395 (Cambrian) and lower (Cambrian-Ordovician and Silurian-Devonian) series is featured
396 by fault breccias, gauges, cataclasites, mylonites, and phyllonites (Fig. 5d). This fault cuts
397 across the (D₁) folded contacts between units located at its hanging wall (Fig. 4a), and
398 produces the juxtaposition of domains showing S₁ fabrics developed under higher
399 metamorphic conditions (biotite-garnet) onto domains either showing colder S₁ fabrics
400 (chlorite-sericite) or non-metamorphic.

401 The fault zone of the Espiel thrust varies in thickness between 5 and 600 meters.
402 Such variation is due to the occurrence of variably-sized fault-bounded domains within
403 the fault zone, some of which reach significant size and lateral continuity as to be
404 represented in regional maps (see lithological description of these rocks in section 3.2).
405 All of the fault-bounded domains that have been mapped show lens-shaped geometry and
406 the upper and lower fault rocks wrapping around these domains exhibit similar kinematic
407 criteria. Out of the fault zone, the hanging wall and footwall maintain internal coherence.
408 The lack of block-in-matrix structure (see section 3.2) suggests an internal imbricate
409 structure for the fault zone of the Espiel thrust.

410 A local planar fabric within the fault zone (S₂) is coincident with the fault zone.
411 Although local obliquity may exist, the angle between internal foliation and border is less
412 than 30°, typically less than 20°. In all cases, the dip direction of tectonic borders and
413 internal foliation is the same. Some differences in orientation can be observed between
414 the borders (and S₂) of the hanging wall and footwall and their internal layering (S₀ and
415 S₁).

416 S₂ is defined by preferred orientation of clasts in fault breccias, by oriented
417 porphyroclasts in cataclasites and mylonites, by mylonitic fabrics, and by C planes in

418 phyllonites formed in metapelitic rocks (Fig. 5d). D₂ kinematic criteria include S-C
419 structures (Fig. 5e), sigma structures (Fig. 5f), and minor drag folds. At the microscopic
420 scale, S₂ is associated with S-C structures, C' shear bands, sigma and delta structures
421 (Fig. 7a), and with the grain-shape alignment of quartz grains oblique to development of
422 S₂ (Fig. 7b). Minerals grown during D₂ include quartz, chlorite and sericite, in
423 metapelites and metaigneous rocks, suggesting D₂ deformation conditions within the
424 upper crust, ranging between low-P/low-T (chlorite) ductile conditions and brittle
425 deformation (gauges and breccias). D₂ kinematic criteria indicate consistent top-to-the-
426 NE shear sense, a vector coincident with the trend of slickensides observed over D₂ fault
427 planes (six confident measurements; Fig. 6d).

428 The cross-cutting relationship between D₁ folds (Espartal syncline) and the D₂
429 Espiel thrust constrains the primary geometry of the thrust relative to that of the folds that
430 now occur at its hanging wall. Most of the upright limb of the Espartal syncline defined
431 by the lowermost metasedimentary rocks (micro-banded phyllites) has been removed by
432 the Espiel thrust in the northeastern exposures of the study area. The reverse limb of the
433 Espartal syncline defined by those same rocks is widely exposed towards the southwest,
434 thus indicating obliquity between D₂ thrust planes and the axial plane of D₁ folds. The
435 asymmetric exposure of D₁ fold limbs relative to the Espiel thrust indicates that the thrust
436 dips steeper than the S₁ axial planes (Fig. 4c), i.e. the Espiel thrust cut upwards to the NE
437 through the D₁ structure.

438 The Espiel thrust is younger than D₁, and is coeval or younger than the Culm
439 facies rocks that are intercalated as fault-bounded domains within the fault zone
440 (Tournaisian – Viséan). The youngest syn-orogenic strata (Peñarroya Beds)
441 unconformably overlie the Espiel thrust, placing a minimum Bashkirian – Moscovian age
442 for D₂.

443

444 **4.3. Upright folds and late thrusts (D₃)**

445 The trace of the Espiel thrust shows a sinuous pattern that reveals its folded nature
446 (Fig. 4a, 4b and 4c). Two D₃ upright folds (Peñarroya antiform and Tejonera synform)
447 affect the Espiel thrust, the bedding in its hanging wall and footwall (Fig. 7c), S₁, and S₂.
448 Pi-diagrams for bedding (Fig. 6a), S₁ (Fig. 6b), and S₂ (Fig. 6d), indicates that D₃ fold
449 axes trend NW-SE and plunge to the SE, parallel to minor D₃ fold axes (Figs. 6e and 7d).
450 Those minor folds are related to a near-vertical (SW-dipping) crenulation cleavage (S₃)
451 that is superimposed on S₁ (Fig. 7d) and S₂ (Fig. 7e), and is parallel to the axial plane of
452 D₃ folds. In metapelites, S₃ is defined by reoriented minerals of S₁ and, locally, S₂, and
453 by newly formed quartz, chlorite, sericite and opaque minerals (low-grade
454 metamorphism). Some Carboniferous syn-orogenics, especially the Culm facies rocks,
455 show a variably developed, near-vertical slaty cleavage that fits with the geometry and
456 mineral composition of S₃. The main and only foliation in those Carboniferous rocks is
457 considered as S₃.

458 The Peñarroya antiform and the Tejonera synform constitute a paired fold
459 structure with two long inclined backlimbs connected by a shorter forelimb (Fig. 4c).
460 Such fold asymmetry implies a local vergence to the NE for D₃ structures. The common
461 limb between the Peñarroya antiform and the Tejonera synform is cut by a NE-directed
462 reverse fault with left-lateral movement (Fig. 4a), as constrained by local exposures of its
463 fault zone. Some meso-scale D₃ folds occur in the footwall to this fault (Peñarroya thrust).
464 Southwest of the Peñarroya thrust, NE-directed thrusts cut across geometrically
465 equivalent upright folds in a similar way (Fig. 4a), suggesting that the latter thrusts and
466 the folds they cut are equivalent to the Peñarroya thrust and D₃ folds, respectively.

467 The Bashkirian – Moscovian Peñarroya Beds cover discordantly the Peñarroya
468 antiform, but are cut by the NE-directed thrusts (Belmez thrust; Figure 4b) and occupy a
469 footwall position relative to the progressively older Carboniferous series that rest on top
470 of them. The Peñarroya Beds are folded by equivalent upright folds to the southwest,
471 suggesting a progressive development for the upright folds and thrusts in the region. The
472 structural relationship and kinematic compatibility between D₃ folds and later NE-
473 directed thrusts fit models for the formation of fault-propagation folds *s.l.* (*Suppe and*
474 *Medwedeff, 1990*). According to the crosscutting relationships observed in the study area,
475 an overstep sequence (younger thrusts to the southwest) of NE-directed thrusts and related
476 folds can be inferred for D₃. The overstep sequence follows the previous development of
477 the D₂ Espiel thrust.

478

479 **5. DISCUSSION**

480 The most salient geological anomaly is the presence of a 600 meters thick tectonic
481 slice of upper mantle (Porvenir serpentinites) emplaced between two blocks with
482 continental affinity that are regionally separated by a single major thrust (Espiel thrust).
483 Such a geological scenario can be considered as a suture zone involving subduction-
484 accretion of the lower tectonic block underneath the slice of upper mantle represented by
485 the Porvenir serpentinites. The upper mantle slice could represent the lowermost part of
486 a dismembered ophiolite *s.l.* (oceanic lithospheric mantle) or the mantle wedge under
487 which subduction took place (subcontinental lithospheric mantle). The lack of continental
488 lower crust (granulitic-eclogitic), plus the absence of a major normal fault to explain the
489 removal of such piece of lower crust, and the lack of block-in-matrix structure within the
490 fault zone (typical for subduction mélanges), suggest a complex evolution. In other

491 words, the obduction of the Porvenir serpentinites was achieved through a multi-step
492 process.

493 A qualitative reconstruction of Variscan structures allows identifying the primary
494 geometry of deformed (e.g., re-folded) structures. Given that the Espiel thrust cut across
495 previous Variscan structures (e.g., D₁ folds), it is expected that this fault has cut other
496 structures. Bearing this in mind, we present a reconstruction of Variscan structures in
497 order to identify the processes involved in the obduction of the Porvenir serpentinites.

498

499 **5.1. Qualitative reconstruction of Variscan structures**

500 The NE-directed tectonic transport of the Espiel thrust imposes an overall SW-
501 dipping component for its main fault plane (*Martínez Poyatos et al.*, 1995b, 1998a). Such
502 paleo-dip-direction would have favored the development of an asymmetric pair of later
503 (D₃) upright folds at the expense of it upon NE-SW shortening, such as the Peñarroya
504 antiform and Tejonera synform (Fig. 4). The crosscutting relationship between the Espiel
505 thrust and D₁ folds implies that D₂ thrust planes had greater SW-dipping values relative
506 to the axial planes of those folds, i.e. the Espiel thrust cut upwards to the NE (see also
507 *Martínez Poyatos et al.*, 1995b). This means that the structural planes of reference (e.g.,
508 axial planes, fault planes, etc.) had either lower SW-dipping values compared to the
509 Espiel thrust, or even dipped to the opposite direction (i.e., to the NE). The NE-vergence
510 of D₁ folds is at odds with a primary NE-dipping geometry, thus a SW-dipping character
511 is inferred for the primary geometry of S₁.

512 Reconstruction of the pre-Espiel thrust structure results in a vertical juxtaposition
513 of fault-bounded terranes in which the Cambrian strata would then occupy the lower
514 structural position. The Porvenir serpentinites, together with some other variably
515 deformed rocks that crop out as fault-bounded domains within the main fault zone, would

516 occupy an intermediate structural position. The Cambrian-Ordovician and Silurian-
517 Devonian strata of the footwall to the Espiel thrust would represent the culmination of the
518 pre-D₂ tectonic pile. This restoration reveals a pre-D₂ tectonic thrust stack with upper
519 mantle rocks (Porvenir serpentinites) sandwiched between two continental tectonic slices.
520 The apparent suture zone was modified by the D₂ thrust. The body of serpentinites is a
521 horse within an imbricate D₂ thrust system, since the current upper and lower boundary
522 of the Porvenir serpentinites are D₂ thrusts that merge to the East and West (Fig. 4a).
523 Such a geometry explains the lack of a lower crust section close to the exposure of the
524 serpentinites (e.g. Fig. 1b), regardless of the primary location of the Porvenir serpentinites
525 either in the subcontinental mantle of the upper plate or as part of oceanic lithosphere in
526 the lower plate.

527 Should the pre-D₂ thrusting event represent a phase of deformation linked to the
528 development of a suture zone, note that its timing matches that of D₁ folds, and both of
529 them account for Devonian contractional tectonics. The D₁ folds were in the footwall to
530 the suture zone and seem coeval to the development of the alleged Devonian suture zone.

531 Studies on the non-coaxial component of deformation associated with D₁
532 (microstructural approach) showed that top-to-the-SE and top-to-the-NW kinematics
533 characterize S₁ (Azor, 1994; *Martínez Poyatos*, 2002). Those shear senses are parallel to
534 D₁ fold axes, what could account for shear strain during fold amplification and lateral
535 spreading linked to superimposed flattening. Petrofabric analyses on S₁ showed that a
536 component of simple shear existed during the development of D₁ folds (Azor, 1994;
537 *Martínez Poyatos*, 2002). The sense of rotation of major forelimbs (vergence) could
538 represent a regional indicator of the shear sense for asymmetric folds generated in relation
539 to simple shear (*Sanderson*, 1979). In this regard, the NE-vergence of D₁ folds is

540 compatible with top-to-the-NE shear sense, i.e. SW-dipping thrust planes and SW-
541 directed subduction polarity for D₁.

542

543 *5.1.1. Regional perspective for a structural reconstruction*

544 Before the Espiel thrust (D₂), the Azuaga Formation exposed in the study area
545 was most probably located under the Porvenir serpentinites, i.e. in the footwall to a
546 Devonian suture zone *s.l.* 20 kilometers southwest of the study area, in the Albarrana
547 Domain (Fig. 3), the Azuaga Formation is in the footwall to a suture zone (*Abalos et al.*,
548 1991b; *Azor et al.*, 1994; *Díez Fernández and Arenas*, 2015; *Pereira et al.*, 2010; *Ribeiro*
549 *et al.*, 2007; *Simancas et al.*, 2003). The suture zone in that area is marked by a high-P
550 metamorphic belt that includes gneisses, micaschists, and mafic rocks (including MORB-
551 type; *Gómez-Pugnaire et al.*, 2003), some of which experienced eclogite facies
552 metamorphism (Central Unit; *Azor et al.*, 1994). High-P metamorphism in the Central
553 Unit is Devonian (377 ± 19 Ma; *Abati et al.*, 2018), and is coincident with the age of D₁
554 folds (see section 4.1).

555 The synchrony between the development of the suture zone exposed in the Central
556 Unit and the development of D₁ folds, and then D₂ thrusts, in the study area, has been
557 explained with a model that acknowledges NE subduction polarity (*Azor et al.*, 1994). In
558 that model, the whole area of study in our work would occupy an upper plate position,
559 the (D₁) NE-verging folds and subsequent (D₂) NE-directed thrusts representing back-
560 folding and associated back-shearing, respectively. That way the upper plate would be
561 subjected to NE-SW shortening upon progressive NE-directed subduction +
562 underthrusting and plate coupling through the subduction zone (*Simancas et al.*, 2001).

563 Previous models are based on the assumption that the Devonian subduction-
564 related high-P metamorphism of the Central Unit was directed to the NE *s.l.* Such

565 assumption finds support in the current NE-dipping geometry of the Central Unit in some
566 areas (*Azor et al.*, 1994; *Simancas et al.*, 2003). However, such models fail to explain
567 why the Azuaga Formation occurs in the upper and lower plate to the suture zone and,
568 more importantly, how a several hundred meters thick tectonic slice of upper mantle
569 (Porvenir serpentinites) could override the upper plate and bring previously folded rocks
570 of the lower plate (Azuaga Formation) along with it. Those models conceive a simple,
571 NE-dipping geometry for the whole Central Unit, based on a seismic profile (*Simancas*
572 *et al.*, 2003) and a field-based structural analysis (*Azor et al.*, 1994) that are restricted to
573 one particular section of the Central Unit. Other structural analyses (e.g., *Abalos et al.*,
574 1991a) and geological maps of the Central Unit (e.g., *Apalategui et al.*, 1982) suggest that
575 the internal structure of that suture zone is controlled by late upright folds (see also *Azor*,
576 1994), the current NE-dipping geometry in some parts being the result of rotation about
577 subhorizontal axes during late upright folding (*Díez Fernández and Arenas*, 2015, 2016).
578 If that is the case, the high-P belt exposed southwest of the study area (Central Unit), and
579 the upper mantle section currently exposed as a tectonic slice within the Espiel thrust,
580 could be (dismembered) parts of the same Devonian suture zone. They both account for
581 individual exposures of a suture zone that share timing (Middle-Late Devonian) and lower
582 plate (Azuaga Formation). The rock association that would account for that suture zone
583 is different in each of its exposures, although some rocks that occur alongside the Porvenir
584 serpentinites could be equivalent to the Central Unit (see section 3.2.3; *Apalategui and*
585 *Pérez-Lorente*, 1983). This implies that at least one mechanism is required to dismember
586 that suture zone.

587 The SW-directed polarity for the Devonian subduction-accretion is supported by
588 the NE-directed vergence of D₁ folds developed in the lower plate and, indirectly, by the
589 regional consequences of a crosscutting relationship between a (D₁) SW-dipping suture

590 zone and later (D₂+D₃) NE-directed thrusts. D₂ and D₃ thrusts cut upwards through
591 previous D₁ structures (see section 4.2). We cannot evaluate quantitatively to what extent
592 D₁ thrust planes rotated by the effect of superimposed thrusting. However, if thrust-
593 related rotation existed, it probably had local consequences only. In other words, if the
594 primary regional dip of D₁ thrust planes was to the SW, that dip would not have changed
595 at the regional scale by D₂ and D₃ thrusts. Accordingly, D₂+D₃ NE-directed thrusts
596 cutting across D₁ SW-dipping thrusts planes (with lower dip values) would allow
597 exposure of D₁ thrusts towards the SW (Figs. 1a-c). On the contrary, should the primary
598 geometry of D₁ thrusts be NE-dipping (NE-directed subduction), superimposed D₂+D₃
599 NE-directed thrusts would have progressively moved the D₁ thrusts to upper structural
600 positions, as to eventually impede their observation to the SW (Figs. 1d-f).

601 The region is characterized by extensional faults (not observed in the study area).
602 The NE-dipping Matachel fault (*Azor et al.*, 1994) separates exposures of the Central Unit
603 to the SW (in its footwall) from the exposures of our study area to the NE (in its hanging
604 wall) (Fig. 3). The down-thrown movement of the NE block of the Matachel fault makes
605 it unlikely that D₁ NE-dipping thrusts in its NE block (Porvenir serpentinites) could be
606 seen in its SW block (Central Unit). Therefore, we conclude that a SW-dipping primary
607 geometry for D₁ thrusts (and for the suture zone they account for) explains the regional
608 concerns.

609 The lower Culm facies (Tournaisian) sequences (see section 3.4.1) suggest that
610 D₁ folding was followed by extension. The resulting vertical juxtaposition of terranes
611 acquired during the previous (D₁) suturing process would be the same. At most, some of
612 the units that once defined the Devonian suture zone would have been removed and/or
613 attenuated before D₂ thrusting, thus introducing another reason why we observe a so
614 dismembered suture zone today.

615

616 **5.2. Tectonic model for the obduction of the Porvenir serpentinites**

617 The structural analysis and qualitative reconstruction of Variscan structures allow
618 a reinterpretation of the Espiel thrust. The model can be summarized in three events: (i)
619 Devonian subduction-accretion directed to the SW (Fig. 8a); (ii) Early Carboniferous out-
620 of-sequence thrusting directed to the NE; (Fig. 8b); and (iii) Late Carboniferous upright
621 folding and thrusting directed to the NE.

622 Deformation in this section of the Variscan orogen started in Devonian times with
623 subduction that involved continental lithosphere (Central Unit) and the upper mantle.
624 Devonian subduction of continental crust gave way to progressive SW-directed
625 underthrusting of continental lithosphere (Azuaga Formation, among others; D₁ folds),
626 which became the lower plate to a suture zone that would include high-P metamorphic
627 rocks with continental crust affinity (Central Unit), ophiolites? (to be found in the study
628 area or nearby), and tectonic slices of upper mantle, either from the overlying mantle
629 wedge of the former subduction zone (continental mantle lithosphere) or from the
630 lowermost part of an ophiolitic ensemble (oceanic mantle lithosphere). The Porvenir
631 serpentinites could potentially account for one of those two options for upper mantle
632 rocks. The upper plate to the Devonian suture zone in the study area would be (at least)
633 the Cambrian-Devonian series exposed in the footwall to the Espiel thrust.

634 After transient extension between D₁ and D₂ (not represented in the model),
635 further SW-directed underthrusting of continental lithosphere during the Early
636 Carboniferous produced steeper and out-of-sequence thrust faults that accommodated
637 shortening. NE-directed D₂ thrusts, such as the Espiel thrust, cut upwards across the
638 overlying Devonian suture zone, thus concluding the obduction of the Porvenir
639 serpentinites (Fig. 8b). The Devonian suture zone was variably dismembered along the

640 imbricate structure of D₂ breaching thrusts, while lower and upper plate switched
641 structural position in the process.

642 Normal faults, such as the Matachel fault, characterized the subsequent stage in
643 the tectonic evolution of SW Iberia. Most of these faults formed during the Carboniferous
644 (late Viséan through to the Bashkirian), and drove lithosphere attenuation by extension
645 (*Dias da Silva et al.*, 2018; *Díez Fernández et al.*, 2019; *Expósito et al.*, 2002; *Pereira et*
646 *al.*, 2009; *Simancas et al.*, 2001).

647 Variscan shortening resumed after Carboniferous extension and affected the
648 whole Iberian Massif during the Bashkirian through to the Gzhelian (*Díez Fernández and*
649 *Pereira*, 2017; *Martínez Catalán et al.*, 2009; *Simancas et al.*, 2001). In the foreland of
650 the orogen, subhorizontal shortening translated into thin-skinned fold-thrust belts, while
651 in the hinterland such shortening was accommodated by strike-slip shear zones and
652 associated upright folds (*Díez Fernández et al.*, 2016). In the study area, NE-SW
653 shortening nucleated upright folds and produced the inversion of Carboniferous
654 sedimentary basins (D₃ thrusts).

655

656 **5.3. Major tectonic implications for the Variscan Orogen in the Iberian Massif**

657 The traditional understanding maintains that the Iberian Massif is an ensemble of
658 continental blocks separated by suture zones, the most relevant of which would be the
659 one that separates the South-Portuguese Zone from the rest of the massif (Fig. 2). That
660 suture has been regarded as a reworked suture zone of the Rheic Ocean (*Azor et al.*, 2008;
661 *Díez Fernández and Arenas*, 2015). The rest of the exposures recognized as Variscan
662 suture zones have been collectively interpreted in two contrasting ways: (i) as correlatives
663 to the Rheic suture zone exposed in SW Iberia (e.g., *Ribeiro et al.*, 2010; *Simancas et al.*,
664 2013); (ii) as secondary suture zones of minor oceanic basins formed in peri-Gondwana

665 at some point during either the opening or closure of the Rheic Ocean (e.g., *Arenas et al.*,
666 2014; *Díez Fernández and Arenas*, 2015; *Simancas et al.*, 2009). Two main models are
667 currently under debate for the second line of thinking. In the one hand, there are models
668 that interpret the exposures of rocks that may represent a Variscan suture zone (high-P
669 rocks, ophiolites, etc.) as the rooting zone for several sutures (e.g., *Azor et al.*, 1994;
670 *Simancas et al.*, 2001), and therefore several continental microblocks other than
671 Gondwana and Laurussia (e.g., *Simancas et al.*, 2009). On the other hand, the model
672 proposed by *Díez Fernández and Arenas* (2015) maintains that most, if not all the
673 exposures of Variscan suture zones other than the one that separates the South-Portuguese
674 Zone from the rest of the Iberian Massif, are actually part of a single, yet dismembered
675 intra-Gondwana suture zone that is rootless and several times repeated across the
676 hinterland of the orogen. This model explains repetition by a combination of faults and
677 late upright folds superimposed to the primary structure of that suture zone. In this view,
678 the latter model recognizes one main continental micro-block besides Gondwana and
679 Laurussia (e.g., Armorica microplate; *Matte*, 2001), and whose boundaries would have
680 been the site for subduction nucleation, accretion and subsequent underthrusting during
681 the Variscan Orogeny (*Díez Fernández et al.*, 2016).

682 Each of the two lines of thinking exposed before has its own implications. If each
683 suture zone exposure accounts for an independent suture zone, there is no need for them
684 to share subduction-accretion polarity. However, they should probably be diachronic
685 (especially in cases where they are few kilometers away from one another), as they would
686 represent the juxtaposition of terranes located across the margins of Gondwana or
687 Laurussia. All the suture zone exposures that separate terranes with Gondwanan affinity
688 in Iberia formed during the Devonian (see revision by *Díez Fernández et al.*, 2016; and
689 recent data by *Abati et al.*, 2018). If there is only one Devonian suture zone that is repeated

690 across the Variscan hinterland, then there should be a way to connect each exposure with
691 the rest throughout the Variscan structure (as tentatively solved by *Díez Fernández and*
692 *Arenas, 2015*). Second, the primary subduction polarity for all the cases must be the same.
693 Our contribution in this regard is that the timing for the formation of the suture zone that
694 is inferred from a qualitative reconstruction of the Espiel thrust fits the age of other
695 independent suture zone exposures that occur elsewhere in the Iberian Massif, and so it
696 does its primary (SW-directed, i.e. Laurussia-directed) subduction-accretion polarity.
697 These two deductions provide further verisimilitude to the single intra-Gondwana suture
698 zone model.

699

700 **6. CONCLUSIONS**

701 The Porvenir serpentinites are a ~600 meters thick body of deformed ultramafic
702 rocks (meta-peridotites) that occurs within a Carboniferous, NE-directed thrust system
703 (Espiel thrust) and affected by upright folds. The obduction of the Porvenir serpentinites
704 was a two-step process: (i) the development of a suture zone during the Devonian; and
705 (ii) the development of the Espiel thrust, which cut across and carried a tectonic slice of
706 upper mantle rocks that belonged to the alleged Devonian suture. Stratigraphic and
707 structural data suggest SW-directed tectonic accretion of the lower plate during the
708 Devonian, and implies Laurussia-directed underthrusting during closure of a Devonian
709 basin that separated two sections of peri-Gondwanan continental crust.

710 The NE-directed nature of the (Carboniferous) Espiel thrust system is compatible
711 with a SW-dipping geometry for the (Devonian) pre-Espiel suture zone. The Porvenir
712 serpentinites and Central Unit are proposed as part of the same suture zone. Late upright
713 folding rotated the Central Unit, as well as other exposures of this Devonian suture zone
714 in the Iberian Massif, to their current geometry. The primary SW-dipping nature of the

715 Devonian suture zone fits the polarity, kinematics and timing of the Late Devonian suture
716 zone that crops out in the Allochthonous Complexes of NW Iberia, and may represent the
717 continuation of such suture zone into SW Iberia.

718

719 **7. ACKNOWLEDGMENTS**

720 Revisions from John Wakabayashi, Stephen Johnston, Francisco Pereira, and an
721 anonymous reviewer contributed to the final version of the manuscript and are highly
722 appreciated. Data available from authors. Color versions of the figures can be found as
723 supplementary material. Supplemental information (Figures 1-8) is available online at
724 XXX. Research funded by Spanish project CGL2016-76438-P (Ministerio de Economía,
725 Industria y Competitividad).

726

727 **8. REFERENCES CITED**

728 Abalos, B., Eguiluz, L., and Gil Ibarguchi, J. I., 1991a, Evolución tectono-metamórfica
729 del Corredor Blastomilonítico de Badajoz-Córdoba. II: Las unidades alóctonas y
730 trayectorias PTt: Boletín Geológico y Minero, v. 102-5, p. 617-671.

731 Abalos, B., Gil Ibarguchi, J. I., and Eguiluz, L., 1991b, Cadomian subduction, collision
732 and Variscan transpression in the Badajoz-Cordoba Shear Belt, Southwest
733 Spain: Tectonophysics, v. 199, p. 51-72.

734 Abati, J., Arenas, R., Díez Fernández, R., Albert, R., and Gerdes, A., 2018, Combined
735 zircon UPb and LuHf isotopes study of magmatism and high-P metamorphism
736 of the basal allochthonous units in the SW Iberian Massif (Ossa-Morena
737 complex): Lithos, v. 322, p. 20-37.

738 Albert, R., Arenas, R., Gerdes, A., Sánchez Martínez, S., Fernández-Suárez, J., and
739 Fuenlabrada, J. M., 2015, Provenance of the Variscan Upper Allochthon (Cabo
740 Ortegual Complex, NW Iberian Massif): Gondwana Research, v. 28, p. 1434-
741 1448.

742 Andreis, R. R., and Wagner, R. H., 1983, Estudio de abanicos aluviales en el norte de la
743 cuenca Wesfaliense B de Peñarroya-Bélmez (Córdoba), in Lemos de Sousa, M.

744 J., ed., Contributions to the Carboniferous Geology and Paleontology of the
745 Iberian Peninsula, Volume 1: Porto, Universidade do Porto, p. 172-227.

746 Apalategui, O., Borrero Domínguez, J., Pérez de la Blanca, J. C., Roldán García, F. J.,
747 Soubrier González, J., and Carracedo, M., 1985, Mapa Geológico, Hoja 902
748 (Adamuz), Serie MAGNA, 1/50.000: Instituto Geológico y Minero de España,
749 Madrid.

750 Apalategui, O., Garrote, A., Roldán García, F. J., and Sánchez Carretero, R., 1982,
751 Mapa Geológico, Hoja 879 (Peñarroya-Pueblonuevo), Serie MAGNA, 1/50.000:
752 Instituto Geológico y Minero de España, Madrid.

753 Apalategui, O., and Pérez-Lorente, F., 1983, Nuevos datos en el borde meridional de la
754 zona centro ibérica : el dominio Obejo-Valsequillo-Puebla de la Reina: *Studia*
755 *Geológica Salmanticensis*, v. 18, p. 193-200.

756 Araújo, A., Fonseca, P. E., Munhá, J. M., Moita, P., Pedro, J., and Ribeiro, A., 2005,
757 The Moura Phyllonitic Complex: an accretionary complex related with
758 obduction in the Southern Iberia Variscan Suture: *Geodinamica Acta*, v. 18, p.
759 375-388.

760 Arenas, R., Díez Fernández, R., Sánchez Martínez, S., Gerdes, A., Fernández-Suárez, J.,
761 and Albert, R., 2014, Two-stage collision: Exploring the birth of Pangea in the
762 Variscan terranes: *Gondwana Research*, v. 25, p. 756-763.

763 Arenas, R., Gil Ibarra, J. I., González Lodeiro, F., Klein, E., Martínez Catalán, J. R.,
764 Ortega Gironés, E., Pablo Maciá, J. G. d., and Peinado, M., 1986,
765 Tectonostratigraphic units in the complexes with mafic and related rocks of the
766 NW of the Iberian Massif: *Hercynica*, v. 2, p. 87-110.

767 Arenas, R., and Sánchez Martínez, S., 2015, Variscan ophiolites in NW Iberia: Tracking
768 lost Paleozoic oceans and the assembly of Pangea: *Episodes*, v. 38, no. 4, p. 315-
769 333.

770 Armendariz, M., López-Guijarro, R., Quesada, C., Pin, C., and Bellido, F., 2008,
771 Genesis and evolution of a syn-orogenic basin in transpression: Insights from
772 petrography, geochemistry and Sm-Nd systematics in the Variscan Pedroches
773 basin (Mississippian, SW Iberia): *Tectonophysics*, v. 461, p. 395-413.

774 Azor, A., 1994, Evolución tectonometamórfica del límite entre las zonas Centroibérica
775 y de Ossa-Morena (Cordillera Varisca, SO de España): Universidad de Granada,
776 312 p.

- 777 Azor, A., González Lodeiro, F., Martínez Poyatos, D., and Simancas, J., 1994a,
778 Regional significance of kilometeric-scale north-east vergent recumbent folds
779 associated with east to south-east directed shear on the southern border of the
780 Central Iberian Zone (Hornachos-Oliva region, Variscan belt, Iberian
781 Peninsula): *Geologische Rundschau*, v. 83, p. 377-387.
- 782 Azor, A., Lodeiro, F. G., and Simancas, J. F., 1994b, Tectonic evolution of the
783 boundary between the Central Iberian and Ossa-Morena zones (Variscan belt,
784 southwest Spain): *Tectonics*, v. 13, p. 45-61.
- 785 Azor, A., Rubatto, D., Simancas, J. F., González Lodeiro, F., Martínez Poyatos, D.,
786 Martín Parra, L. M., and Matas, J., 2008, Rheic Ocean ophiolitic remnants in
787 southern Iberia questioned by SHRIMP U-Pb zircon ages on the Beja-
788 Acebuches amphibolites: *Tectonics*, v. 27, p. TC5006.
- 789 Bellon, H., Blachere, H., Crousilles, M., Deloche, C., Dixsaut, C., Hertricht, B., Prost-
790 Dame, V., Rossi, P., Simon, D., and Tamain, G., 1979, Radiochronologie,
791 évolution tectonomagmatique et implications métallogéniques dans les Cadomo-
792 variscides du Sud-Est Hespérique: *Bulletin de la Societe Geologique de France*,
793 v. 21, p. 113-120.
- 794 Blatrix, P., and Burg, J. P., 1981, $^{40}\text{Ar}/^{39}\text{Ar}$ dates from Sierra Morena (southern
795 Spain): Variscan metamorphism and Cadomian Orogeny: *Neues Jahrbuch*
796 *Mineral Monatshefte*, v. 10, p. 470-478.
- 797 Carracedo, M., Paquette, J. L., Olazabal, A. A., Santos Zalduegui, J. F., de
798 Madinabeitia, S. G., Tiepolo, M., and Gil Ibarguchi, J. I., 2009, U-Pb dating of
799 granodiorite and granite units of the Los Pedroches batholith. Implications for
800 geodynamic models of the southern Central Iberian Zone (Iberian Massif):
801 *International Journal of Earth Sciences*, v. 98, p. 1609-1624.
- 802 Coleman, R. G., 1981, Tectonic setting for ophiolite obduction in Oman: *Journal of*
803 *Geophysical Research: Solid Earth*, v. 86, no. B4, p. 2497-2508.
- 804 Corfield, R. I., Searle, M. P., and Pedersen, R. B., 2001, Tectonic Setting, Origin, and
805 Obduction History of the Spontang Ophiolite, Ladakh Himalaya, NW India: *The*
806 *Journal of Geology*, v. 109, no. 6, p. 715-736.
- 807 Chichorro, M., Pereira, M. F., Díaz-Azpiroz, M., Williams, I. S., Fernández, C., Pin, C.,
808 and Silva, J. B., 2008, Cambrian ensialic rift-related magmatism in the Ossa-
809 Morena Zone (Évora-Aracena metamorphic belt, SW Iberian Massif): Sm-Nd

810 isotopes and SHRIMP zircon U–Th–Pb geochronology: *Tectonophysics*, v. 461,
811 p. 91-113.

812 Dallmeyer, R. D., and Quesada, C., 1992, Cadomian vs. Variscan evolution of the Ossa-
813 Morena zone (SW Iberia): field and $^{40}\text{Ar}/^{39}\text{Ar}$ mineral age constraints:
814 *Tectonophysics*, v. 216, p. 339-364.

815 Delgado Quesada, M., 1971, Esquema Geológico de la hoja No. 878 de Azuaga
816 (Badajoz): *Boletín Geológico Minero*, v. 82, p. 277-286.

817 Dewey, J. F., 1976, Ophiolite obduction: *Tectonophysics*, v. 31, p. 93-120.

818 Dias da Silva, Í., Pereira, M. F., Silva, J. B., and Gama, C., 2018, Time-space
819 distribution of silicic plutonism in a gneiss dome of the Iberian Variscan Belt:
820 The Évora Massif (Ossa-Morena Zone, Portugal): *Tectonophysics*, v. 747-748,
821 p. 298-317.

822 Díez Fernández, R., and Arenas, R., 2015, The Late Devonian Variscan suture of the
823 Iberian Massif: A correlation of high-pressure belts in NW and SW Iberia:
824 *Tectonophysics*, v. 654, p. 96-100.

825 -, 2016, Reply to Comment on “The Late Devonian Variscan suture of the Iberian
826 Massif: A correlation of high-pressure belts in NW and SW Iberia”:
827 *Tectonophysics*, v. 670, p. 155-160.

828 Díez Fernández, R., Arenas, R., Pereira, M. F., Sánchez Martínez, S., Albert, R., Martín
829 Parra, L. M., Rubio Pascual, F. J., and Matas, J., 2016, Tectonic evolution of
830 Variscan Iberia: Gondwana - Laurussia collision revisited: *Earth-Science*
831 *Reviews*, v. 162, p. 269-292.

832 Díez Fernández, R., Fuenlabrada, J. M., Chichorro, M., Pereira, M. F., Sánchez
833 Martínez, S., Silva, J. B., and Arenas, R., 2017, Geochemistry and
834 tectonostratigraphy of the basal allochthonous units of SW Iberia (Évora Massif,
835 Portugal): keys to the reconstruction of pre-Pangean paleogeography in southern
836 Europe: *Lithos*, v. 268-271, p. 285-301.

837 Díez Fernández, R., Jiménez-Díaz, A., Arenas, R., Pereira, M. F., and Fernández-
838 Suárez, J., 2019, Ediacaran Obduction of a Fore-arc Ophiolite in SW Iberia: A
839 Turning Point in the Evolving Geodynamic Setting of Peri-Gondwana:
840 *Tectonics*, v. 38, p. 95-119.

841 Díez Fernández, R., Martínez Catalán, J. R., Arenas, R., and Abati, J., 2011, Tectonic
842 evolution of a continental subduction-exhumation channel: Variscan structure of
843 the basal allochthonous units in NW Spain: *Tectonics*, v. 30, p. TC3009.

844 Díez Fernández, R., Martínez Catalán, J. R., Arenas, R., and Abati, J., 2012, The onset
845 of the assembly of Pangaea in NW Iberia: Constraints on the kinematics of
846 continental subduction: *Gondwana Research*, v. 22, p. 20-25.

847 Díez Fernández, R., Martínez Catalán, J. R., Gerdes, A., Abati, J., Arenas, R., and
848 Fernández-Suárez, J., 2010, U–Pb ages of detrital zircons from the Basal
849 allochthonous units of NW Iberia: Provenance and paleoposition on the northern
850 margin of Gondwana during the Neoproterozoic and Paleozoic: *Gondwana
851 Research*, v. 18, p. 385-399.

852 Díez Fernández, R., and Pereira, M. F., 2017, Strike-slip shear zones of the Iberian
853 Massif: are they coeval?: *Lithosphere*, v. 9, no. 5, p. 726-744.

854 Dilek, Y., and Furnes, H., 2014, Ophiolites and Their Origins: *Elements*, v. 10, no. 2, p.
855 93-100.

856 Eguíluz, L., Gil Ibarra, J. I., Abalos, B., and Apraiz, A., 2000, Superposed
857 Hercynian and Cadomian orogenic cycles in the Ossa-Morena zone and related
858 areas of the Iberian Massif: *Geological Society of America Bulletin*, v. 112, p.
859 1398-1413.

860 Expósito, I., Simancas, J. F., González Lodeiro, F., Azor, A., and Martínez Poyatos, D.
861 J., 2002, La estructura de la mitad septentrional de la Zona de Ossa-Morena:
862 deformación en el bloque inferior de un cabalgamiento cortical de evolución
863 compleja: *Revista de la Sociedad Geológica de España*, v. 15, p. 3-14.

864 Garrote, A., and Broutin, J., 1979, Le bassin toumaisien de Benajarafe (Province de
865 Cordoue, Espagne). *Géologie et premières données paléobotaniques et
866 palynologiques: Comptes Rendus du 104 Congrès national des Sociétés savantes
867 (Bordeaux)*, v. 1, p. 175-184.

868 Godfrey, N. J., Beaudoin, B. C., and Klemperer, S. L., 1997, Ophiolitic basement to the
869 Great Valley forearc basin, California, from seismic and gravity data:
870 Implications for crustal growth at the North American continental margin:
871 *Geological Society of America Bulletin*, v. 109, no. 12, p. 1536-1562.

872 Gómez-Pugnaire, M.T., Azor, A., Fernández-Soler, J.M., and Sánchez-Vizcaíno, V.L.,
873 2003, The amphibolites from the Ossa–Morena/Central Iberian Variscan suture
874 (Southwestern Iberian Massif): geochemistry and tectonic interpretation: *Lithos*,
875 v. 68, p. 23-42.

876 Gutiérrez-Marco, J. C., Robardet, M., Rábano, I., Sarmiento, G. N., San José Lancha,
877 M. A., Herranz Araujo, P., and Pieren Pidal, A. P., 2002, Ordovician, in

- 878 Gibbons, W., and Moreno, T., eds., *The Geology of Spain*: London, Geological
879 Society of London, p. 31-49.
- 880 Jensen, S., Palacios, T., Eguiluz, L., 2004, Cambrian ichnofabrics from the Ossa
881 Morena and Central Iberian zones: preliminary results: *Geo-Temas*, v. 6, no. 2,
882 p. 291-293.
- 883 Linnemann, U., Pereira, F., Jeffries, T. E., Drost, K., and Gerdes, A., 2008, The
884 Cadomian Orogeny and the opening of the Rheic Ocean: The diacrony of
885 geotectonic processes constrained by LA-ICP-MS U–Pb zircon dating (Ossa-
886 Morena and Saxo-Thuringian Zones, Iberian and Bohemian Massifs):
887 *Tectonophysics*, v. 461, p. 21-43.
- 888 Liñán, E., 1978, *Bioestratigrafía de la Sierra de Córdoba* [PhD]: Universidad de
889 Granada, 212 p.
- 890 Liñán, E., and Quesada, C., 1990, Ossa-Morena Zone: 2. Stratigraphy. Rift phase, in
891 Dallmeyer, R. D., and Martínez García, E., eds., *Pre-Mesozoic Geology of*
892 *Iberia*: Berlin, Germany, Springer- Verlag, p. 259–266.
- 893 López Munguira, A., Nieto, F., Sebastián Pardo, E., and Velilla, N., 1991, The
894 composition of phyllosilicates in Precambrian, low-grademetamorphic, clastic
895 rocks from the Southern Hesperian Massif (Spain) used as an indicator to
896 metamorphic conditions: *Precambrian Research*, v. 53, no. 3, p. 267-279.
- 897 Llopis, N., San José, M. A., and Herranz, P., 1970, Notas sobre una discordancia
898 posiblemente precámbrica al SE de la provincia de Badajoz y sobre la edad de
899 las series paleozoicas circundantes: *Boletín Geológico Minero*, v. 81, p. 586-
900 592.
- 901 Mamet, B., and Martínez, C., 1981, Late Vissean microfossils of the Las Caleras Bajas
902 limestone (Córdoba, Spain): *Revista Española de Micropaleontología*, v. 13, p.
903 105-118.
- 904 Martín Parra, L. M., González Lodeiro, F., Martínez Poyatos, D., and Matas, J., 2006,
905 The Puente Génave–Castelo de Vide Shear Zone (southern Central Iberian Zone,
906 Iberian Massif): geometry, kinematics and regional implications: *Bulletin de la*
907 *Société Géologique de France*, v. 177, p. 191-202.
- 908 Martínez Catalán, J. R., 1990, A non-cylindrical model for the northwest Iberian
909 allochthonous terranes and their equivalents in the Hercynian belt of Western
910 Europe: *Tectonophysics*, v. 179, p. 253-272.

- 911 Martínez Catalán, J. R., Arenas, R., Abati, J., Sánchez Martínez, S., Díaz García, F.,
912 Fernández-Suárez, J., González Cuadra, P., Castiñeiras, P., Gómez Barreiro, J.,
913 Díez Montes, A., González Clavijo, E., Rubio Pascual, F. J., Andonaegui, P.,
914 Jeffries, T. E., Alcock, J. E., Díez Fernández, R., and López Carmona, A., 2009,
915 A rootless suture and the loss of the roots of a mountain chain: The Variscan belt
916 of NW Iberia: *Comptes Rendus Geoscience*, v. 341, p. 114-126.
- 917 Martínez Catalán, J. R., Arenas, R., Díaz García, F., Gómez Barreiro, J., González
918 Cuadra, P., Abati, J., Castiñeiras, P., Fernández-Suárez, J., Sánchez Martínez, S.,
919 Andonaegui, P., González Clavijo, E., Díez Montes, A., Rubio Pascual, F. J.,
920 and Valle Aguado, B., 2007, Space and time in the tectonic evolution of the
921 northwestern Iberian Massif. Implications for the Variscan belt, in Hatcher, R.
922 D., Carlson, M. P., McBride, J. H., and Martínez Catalán, J. R., eds., 4-D
923 Framework of Continental Crust, Volume 200: Boulder, Colorado, Geological
924 Society of America Memoir, p. 403-423.
- 925 Martínez Catalán, J. R., Arenas, R., Díaz García, F., Rubio Pascual, F. J., Abati, J., and
926 Marquín García, J., 1996, Variscan exhumation of a subducted paleozoic
927 continental margin: The basal units of the Ordenes Complex, Galicia, NW
928 Spain: *Tectonics*, v. 15, p. 106-121.
- 929 Martínez Poyatos, D., Azor, A., González Lodeiro, F., and Simancas, J. F., 1995a,
930 Timing of the Variscan structures on both sides of the Ossa-Morena/Central
931 Iberian contact (southwest Iberian Massif): *Comptes Rendus de l'Académie des*
932 *Sciences de Paris*, v. 321, p. 609-615.
- 933 Martínez Poyatos, D., Carbonell, R., Palomeras, I., Simancas, J. F., Ayarza, P., Martí,
934 D., Azor, A., Jabaloy, A., González Cuadra, P., Tejero, R., Martín Parra, L. M.,
935 Matas, J., González Lodeiro, F., Pérez-Estaún, A., García Lobón, J. L., and
936 Mansilla, L., 2012, Imaging the crustal structure of the Central Iberian Zone
937 (Variscan Belt): The ALCUDIA deep seismic reflection transect: *Tectonics*, v.
938 31, p. TC3017.
- 939 Martínez Poyatos, D., González Lodeiro, F., Azor, A., and Simancas, J. F., 2001, La
940 estructura de la Zona Centroibérica en la región de Los Pedroches (Macizo
941 Ibérico meridional): *Revista de la Sociedad Geológica de España*, v. 14, p. 147-
942 160.
- 943 Martínez Poyatos, D., Simancas, J. F., Azor, A., and González Lodeiro, F., 1995b, La
944 estructura del borde meridional de la Zona Centroibérica en el sector suroriental

945 de la Provincia de Badajoz: Revista de la Sociedad Geológica de España, v. 8, p.
946 41-50.

947 -, 1998a, Evolution of a Carboniferous piggyback basin in the southern Central Iberian
948 Zone (Variscan Belt, SE Spain): Bulletin de la Société Géologique de France, v.
949 169, p. 573-578.

950 -, 1998b, La estructura del borde meridional de la Zona Centroibérica (Macizo Ibérico)
951 en el Norte de la Provincia de Córdoba: Revista de la Sociedad Geológica de
952 España, v. 11, p. 87-94.

953 Martínez Poyatos, D. J., 2002, Estructura del borde meridional de la Zona Centroibérica
954 y su relación con el contacto entre las Zonas Centroibérica y de Ossa-Morena:
955 Nova Terra, v. 18, p. 1-295.

956 Mata, J., and Munhá, J., 1986, Geodynamic significance of high-grade metamorphic
957 rocks from Degolados-Campo Maior (Tomar-Badajoz-Córdoba shear zone):
958 Maleo, v. 2, p. 28.

959 Matas, J., Martín Parra, L. M., and Martínez Poyatos, D., 2015a, Mapa y Memoria del
960 Mapa Geológico Nacional a escala 1:200.000 (MAGE200) nº 69 (Pozoblanco):
961 Instituto Geológico y Minero de España.

962 Matas, J., Martín Parra, L. M., Roldán, F. J., and Martín-Serrano, A., 2015b, Mapa y
963 Memoria del Mapa Geológico Nacional a escala 1:200.000 (MAGE200) nº 76
964 (Córdoba): Instituto Geológico y Minero de España.

965 Matte, P., 2001, The Variscan collage and orogeny (480-290 Ma) and the tectonic
966 definition of the Armorica microplate: a review: Terra Nova, v. 13, p. 122-128.

967 Ortuño, M. G., 1971, Middle Westphalian strata in South-West Spain: Proceedings of
968 the VII Congr. Intern. Strat. Géol. Carbonif. (Sheffield, 1967), v. 3, p. 1275-
969 1292.

970 Pereira, M. F., Apraiz, A., Chichorro, M., Silva, J. B., and Armstrong, R. A., 2010,
971 Exhumation of high-pressure rocks in northern Gondwana during the Early
972 Carboniferous (Coimbra-Cordoba shear zone, SW Iberian Massif):
973 Tectonothermal analysis and U–Th–Pb SHRIMP in-situ zircon geochronology:
974 Gondwana Research, v. 17, p. 440-460.

975 Pereira, M. F., Chichorro, M., Williams, I. S., Silva, J. B., Fernández, C., Díaz-Azpiroz,
976 M., Apraiz, A., and Castro, A., 2009, Variscan intra-orogenic extensional
977 tectonics in the Ossa-Morena Zone (Évora-Aracena-Lora del Río metamorphic

978 belt, SW Iberian Massif): SHRIMP zircon U–Th–Pb geochronology: Geological
979 Society, London, Special Publications, v. 327, p. 215-237.

980 Pérez-Cáceres, I., Simancas, J. F., Martínez Poyatos, D., Azor, A., and González
981 Lodeiro, F., 2016, Oblique collision and deformation partitioning in the SW
982 Iberian Variscides: *Solid Earth*, v. 7, p. 857-872.

983 Pérez Lorente, F., 1979, Geología de la Zona de Ossa-Morena al norte de Córdoba
984 (Pozoblanco-Belmez-Villaviciosa de Córdoba)PhD]: Universidad de Granada,
985 340 p.

986 Ribeiro, A., Munhá, J., Dias, R., Mateus, A., Pereira, E., Ribeiro, L., Fonseca, P.,
987 Araújo, A., Oliveira, T., Romão, J., Chaminé, H., Coke, C., and Pedro, J., 2007,
988 Geodynamic evolution of the SW Europe Variscides: *Tectonics*, v. 26, p.
989 TC6009.

990 Ribeiro, A., Munhá, J., Fonseca, P. E., Araújo, A., Pedro, J. C., Mateus, A., Tassinari,
991 C., Machado, G., and Jesus, A., 2010, Variscan ophiolite belts in the Ossa-
992 Morena Zone (Southwest Iberia): Geological characterization and geodynamic
993 significance: *Gondwana Research*, v. 17, p. 408-421.

994 Ribeiro, A., Pereira, E., and Dias, R., 1990, Structure in the northwest of the Iberian
995 Peninsula, in Dallmeyer, R. D., and Martínez García, E., eds., *Pre-Mesozoic
996 Geology of Iberia*: Berlin, Germany, Springer-Verlag, p. 220-236.

997 Robardet, M., and Gutiérrez Marco, J. C., 2004, The Ordovician, Silurian and Devonian
998 sedimentary rocks of the Ossa-Morena Zone (SW Iberian Peninsula, Spain):
999 *Journal of Iberian Geology*, v. 30, p. 73-92.

1000 Robertson, A. H. F., 2006, Contrasting modes of ophiolite emplacement in the Eastern
1001 Mediterranean region: *Geological Society, London, Memoirs*, v. 32, no. 1, p.
1002 235-261.

1003 Sánchez-García, T., Bellido, F., and Quesada, C., 2003, Geodynamic setting and
1004 geochemical signatures of Cambrian–Ordovician rift-related igneous rocks
1005 (Ossa-Morena Zone, SW Iberia): *Tectonophysics*, v. 365, p. 233-255.

1006 Sanderson, D. J., 1979, The transition from upright to recumbent folding in the Variscan
1007 fold belt of southwest England: a model based on the kinematics of simple shear:
1008 *Journal of Structural Geology*, v. 1, no. 3, p. 171-180.

1009 Simancas, J. F., Ayarza, P., Azor, A., Carbonell, R., Martínez Poyatos, D., Pérez-
1010 Estaún, A., and González Lodeiro, F., 2013, A seismic geotraverse across the

- 1011 Iberian Variscides: Orogenic shortening, collisional magmatism, and orocline
1012 development: *Tectonics*, v. 32, p. 417-432.
- 1013 Simancas, J. F., Azor, A., Martínez-Poyatos, D., Tahiri, A., El Hadi, H., González-
1014 Lodeiro, F., Pérez-Estaún, A., and Carbonell, R., 2009, Tectonic relationships of
1015 Southwest Iberia with the allochthons of Northwest Iberia and the Moroccan
1016 Variscides: *Comptes Rendus Geoscience*, v. 341, p. 103-113.
- 1017 Simancas, J. F., Carbonell, R., González Lodeiro, F., Pérez Estaún, A., Juhlin, C.,
1018 Ayarza, P., Kashubin, A., Azor, A., Martínez Poyatos, D., Almodóvar, G. R.,
1019 Pascual, E., Sáez, R., and Expósito, I., 2003, Crustal structure of the
1020 transpressional Variscan orogen of SW Iberia: SW Iberia deep seismic reflection
1021 profile (IBERSEIS): *Tectonics*, v. 22, p. 1062.
- 1022 Simancas, J. F., Martínez Poyatos, D., Expósito, I., Azor, A., and González Lodeiro, F.,
1023 2001, The structure of a major suture zone in the SW Iberian Massif: the Ossa-
1024 Morena/Central Iberian contact: *Tectonophysics*, v. 332, p. 295-308.
- 1025 Suppe, J., and Medwedeff, D. A., 1990, Geometry and kinematics of fault-propagation
1026 folding: *Eclogae Geologicae Helvetiae*, v. 83, no. 3, p. 409-454.
- 1027 Talavera, C., Martínez Poyatos, D., and González Lodeiro, F., 2015, SHRIMP U–Pb
1028 geochronological constraints on the timing of the intra-Alcudian (Cadomian)
1029 angular unconformity in the Central Iberian Zone (Iberian Massif, Spain):
1030 *International Journal of Earth Sciences*, v. 104, no. 7, p. 1739-1757.
- 1031 Topuz, G., Çelık, Ö. F., Şengör, A. M. C., Altıntaş, İ. E., Zack, T., Rolland, Y., and
1032 Barth, M., 2013, Jurassic ophiolite formation and emplacement as backstop to a
1033 subduction-accretion complex in northeast Turkey, the Refahiye ophiolite, and
1034 relation to the Balkan ophiolites: *American Journal of Science*, v. 313, no. 10, p.
1035 1054-1087.
- 1036 Wagner, R. H., 2004, The Iberian Massif: a Carboniferous assembly: *Journal of Iberian
1037 Geology*, v. 30, p. 93-108.

1038

1039 **FIGURE CAPTION**

1040 **Figure 1:** Cartoon showing the upper and lower block of a suture zone switching places
1041 by superimposed NE-directed thrusting. Sections (a), (b) and (c) show a case example for
1042 a primary SW-dipping suture zone, whereas sections (d), (e) and (f) represent the case for

1043 a NE-dipping suture zone. Note that forward modelling from (a) to (c) provide several
1044 possibilities for a primary SW-dipping suture zone to occur (stars) towards the SW of a
1045 series of NE-directed thrusts (e.g., Espiel thrust) and normal faults (e.g., Matachel fault)
1046 with down-thrown movement of their NE block, whereas that possibility is much less
1047 likely in the case of a primary NE-dipping geometry for the suture zone (forward
1048 modelling from (d) to (f)). Dip values and crosscutting relationships are not intended to
1049 reproduce those of the study case. The primary geometry of the suture zone is
1050 oversimplified (rather continuous and tabular-shaped) for clarity.

1051

1052 **Figure 2:** Zonation and major tectonic elements of the Iberian Massif after *Díez*
1053 *Fernández and Arenas* (2015). Abbreviations: AF — Azuaga Fault; BToIP — Basal
1054 Thrust of the Iberian Parautochthon; BAO — Beja–Acebuches Ophiolite; CA —
1055 Carvalhal Amphibolites; CF — Canaleja Fault; CMU — Cubito–Moura Unit; CO —
1056 Calzadilla Ophiolite; CU — Central Unit; EsT — Espiel Thrust; ET—Espina Thrust;
1057 HF— Hornachos Fault; IOMZO —Internal Ossa-Morena Zone Ophiolites; J-PCSZ —
1058 Juzbado-Penalva do Castelo Shear Zone; LFT — Lalín-Forcarei Thrust; LPSZ — Los
1059 Pedroches Shear Zone; LLSZ — Llanos Shear Zone; MLSZ — Malpica–Lamego Shear
1060 Zone; MF — Matachel Fault; OF — Onza Fault; OVD — Obejo–Valsequillo Domain;
1061 PG–CVD — Puente Génave–Castelo de Vide Detachment; PRSZ— Palas de Rei Shear
1062 Zone; PTSZ — Porto–Tomar Shear Zone; RF — Riás Fault; SISZ —South Iberian Shear
1063 Zone; VF — Viveiro Fault; ZSI — Zalamea de la Serena Imbricates.

1064

1065 **Figure 3:** Geological map of the Obejo-Valsequillo Domain (see location in Figure 2).
1066 Regional synthesis based on maps published by the Spanish Geological Survey (*Matas et*
1067 *al.*, 2015a, 2015b, and references therein), *Martínez Poyatos et al.* (2012), and our own

1068 data. The Espiel thrust has been discriminated from the rest of the thrusts of the region
1069 due to its bearing on the geology of the study area and on the discussion presented in this
1070 work.

1071

1072 **Figure 4:** (a) Geological map and (b and c) cross-sections of the study area (see regional
1073 location in Figure 3). Names of main structures referred to in the text are indicated in
1074 cross-sections.

1075

1076 **Figure 5:** (a) Field exposure of the Porvenir serpentinites. Note their general massive
1077 aspect and spaced planar anisotropy (S_n). (b) Thin-section to the Porvenir serpentinites.
1078 Note olivine being replaced by serpentine and the presence of spinel. Olivine was the
1079 major constituent of this meta-peridotite, likely a serpentitized dunite. (c) Crosscutting
1080 relationship between bedding (S_0) and S_1 in the Azuaga Formation. (d) Phyllonites within
1081 the fault zone of the Espiel thrust. (e) S-C structures in phyllonites within the fault zone
1082 of the Espiel thrust (top-to-the-NE shear sense). (f) Porphyritic metagranitoid showing
1083 sigma structures defined by a quartz porphyroclast and a K-feldspar porphyroclast
1084 (undifferentiated metaigneous rocks) surrounded by mylonitic foliation (S_2) within the
1085 fault zone of the Espiel thrust (top-to-the-NE shear sense). The absence of lens-shaped,
1086 highly stretched layers rich in feldspar or quartz in these rocks suggest that most of the
1087 mylonitic foliation was likely developed at the expense of the ground mass of a
1088 porphyritic granitoid.

1089

1090 **Figure 6:** Pi-diagrams constructed for (a) bedding and (b) S_1 . (c) Stereoplot showing the
1091 orientation of D_1 intersection lineation between S_0 - S_1 (L_1). (d) Pi-diagram for S_2 and

1092 shear sense and orientation of D₂ slickensides. (e) Stereoplot showing the orientation of
1093 D₃ fold axes (F₃).

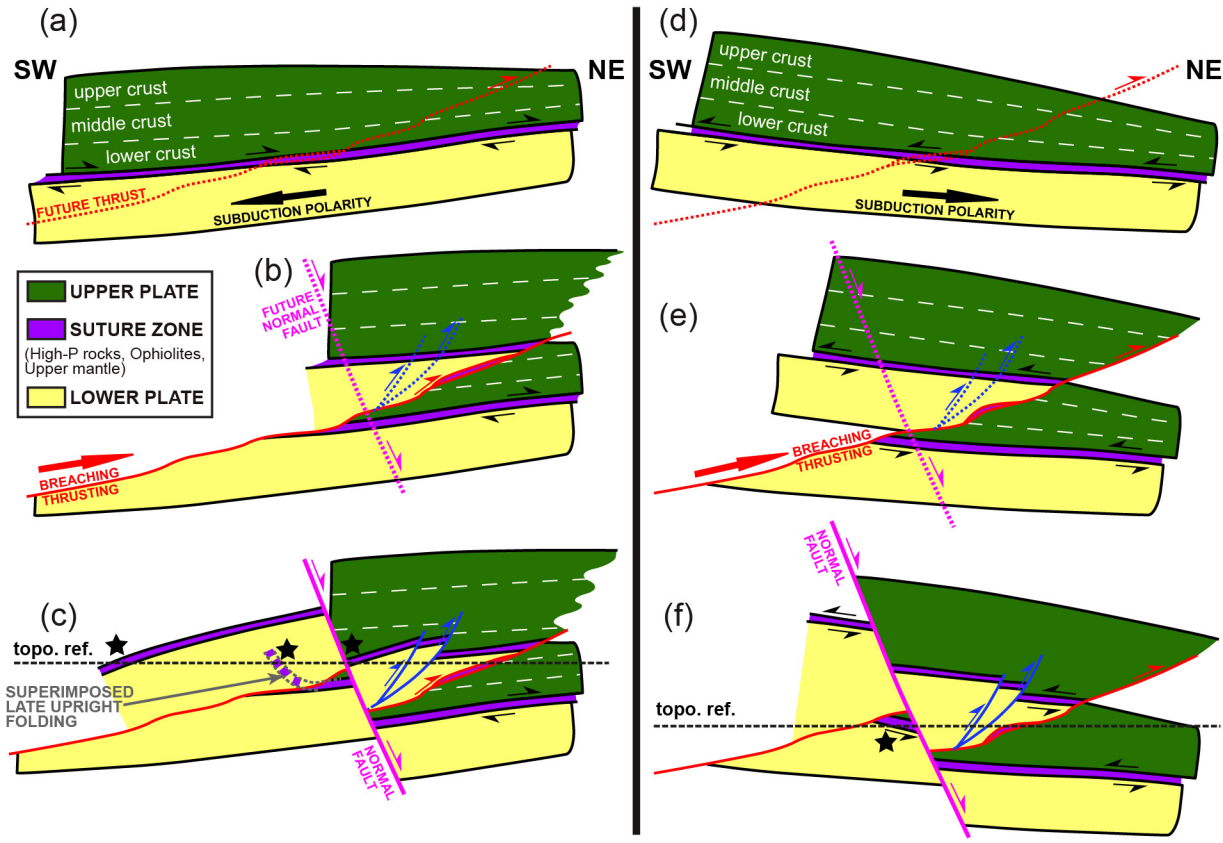
1094

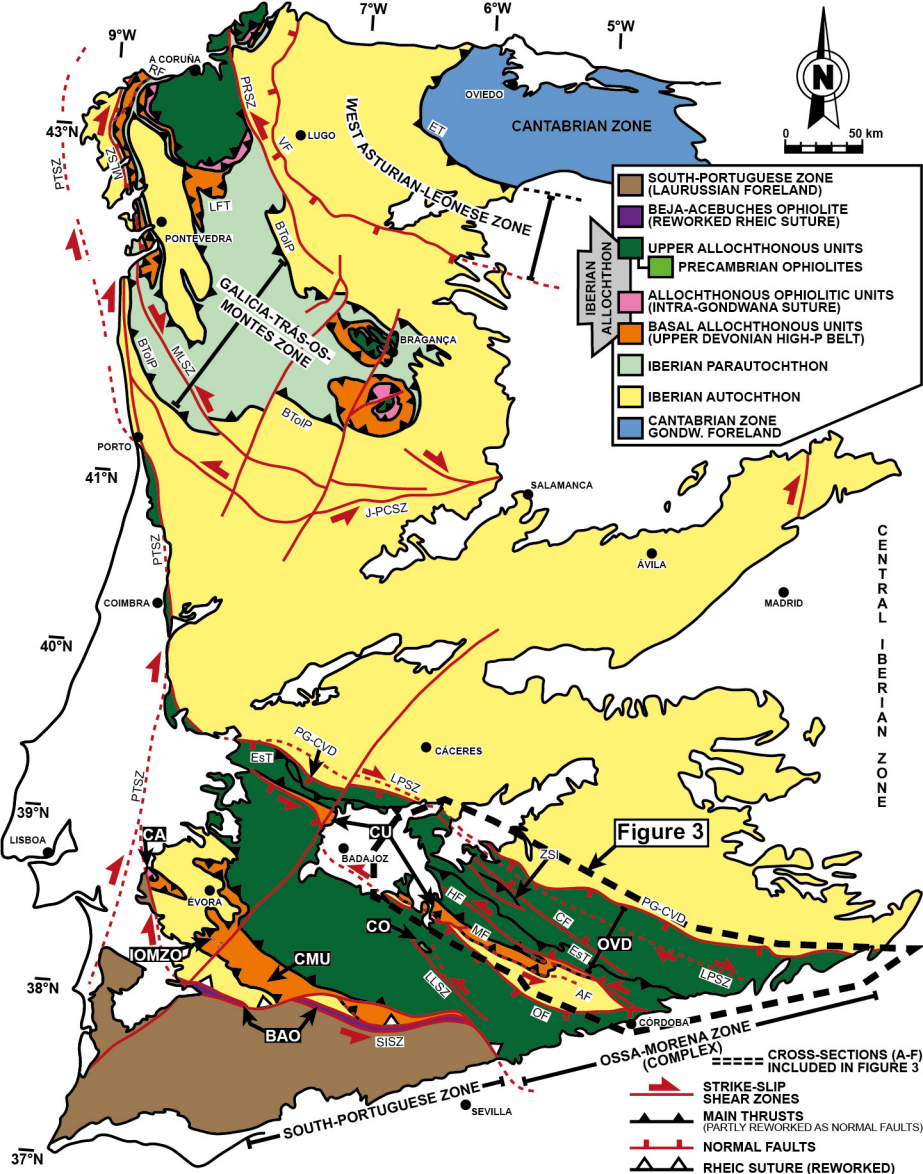
1095 **Figure 7:** (a) Sigma (σ) and delta (δ) structures associated with S₂ (top-to-the-NE) in
1096 mylonites within the Espiel thrust. (b) Shape fabric defined by quartz subgrains (yellow
1097 line) oblique to S₂ (top-to-the-NE) in mylonites within the Espiel thrust. (c) Panoramic
1098 view of the Peñarroya antiform. Cambrian-Ordovician metasandstone layers show the
1099 local dip direction for each fold limb. Picture taken from Pueblonuevo village and looking
1100 to the NW. (d) D₃ minor upright folds affecting S₁ (Azuaga Formation). Note incipient
1101 S₃ crenulation cleavage. (e) D₃ upright folds affecting a mylonitic fabric (S₂) within the
1102 fault zone of the Espiel thrust. S₂ in this porphyritic metagranitoid includes sigma
1103 structures defined by K-feldspar porphyroclasts indicating top-to-the-NE shear sense.

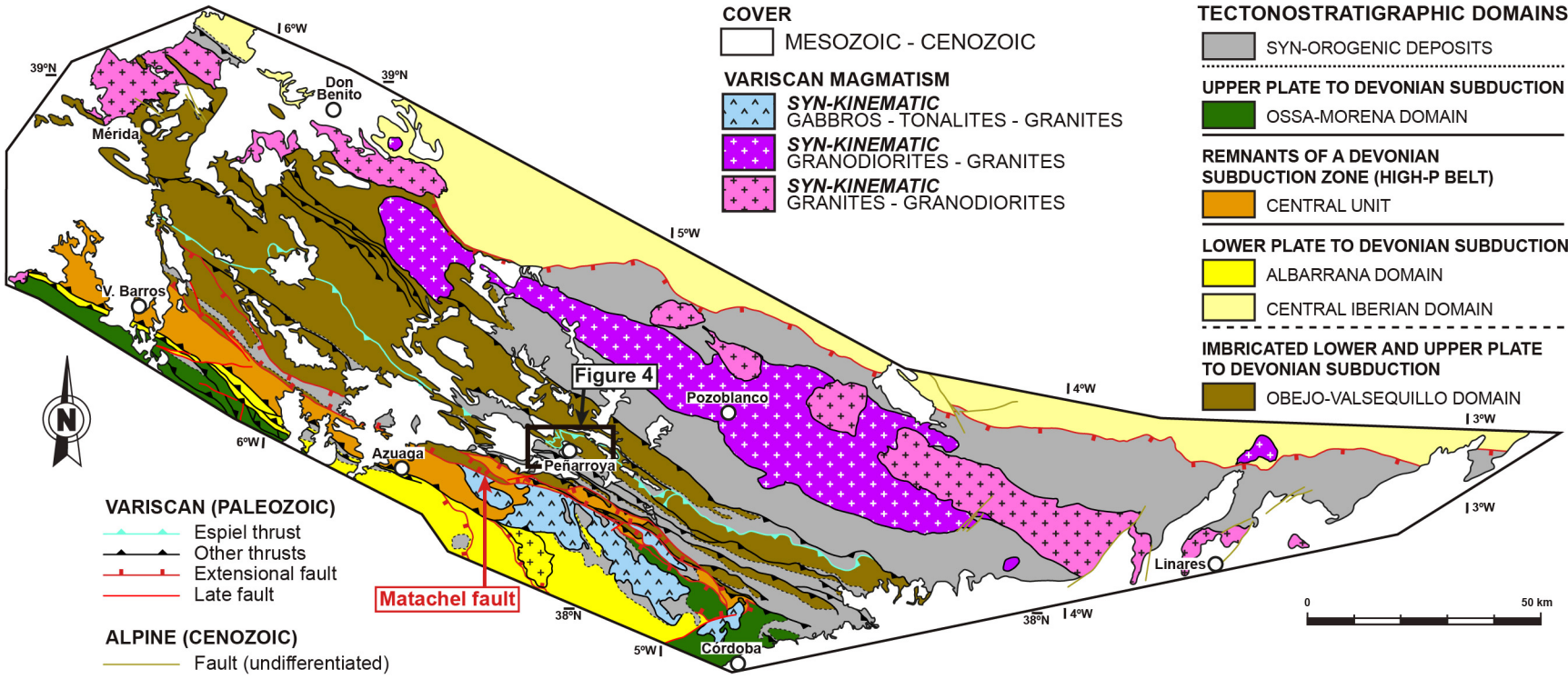
1104

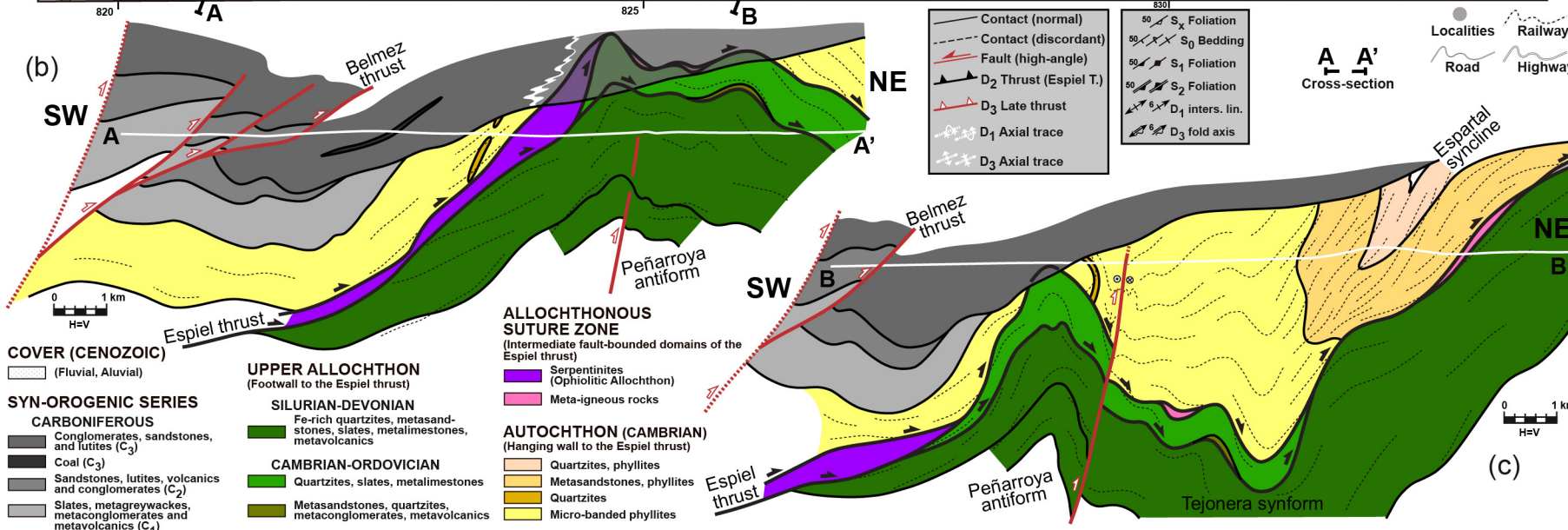
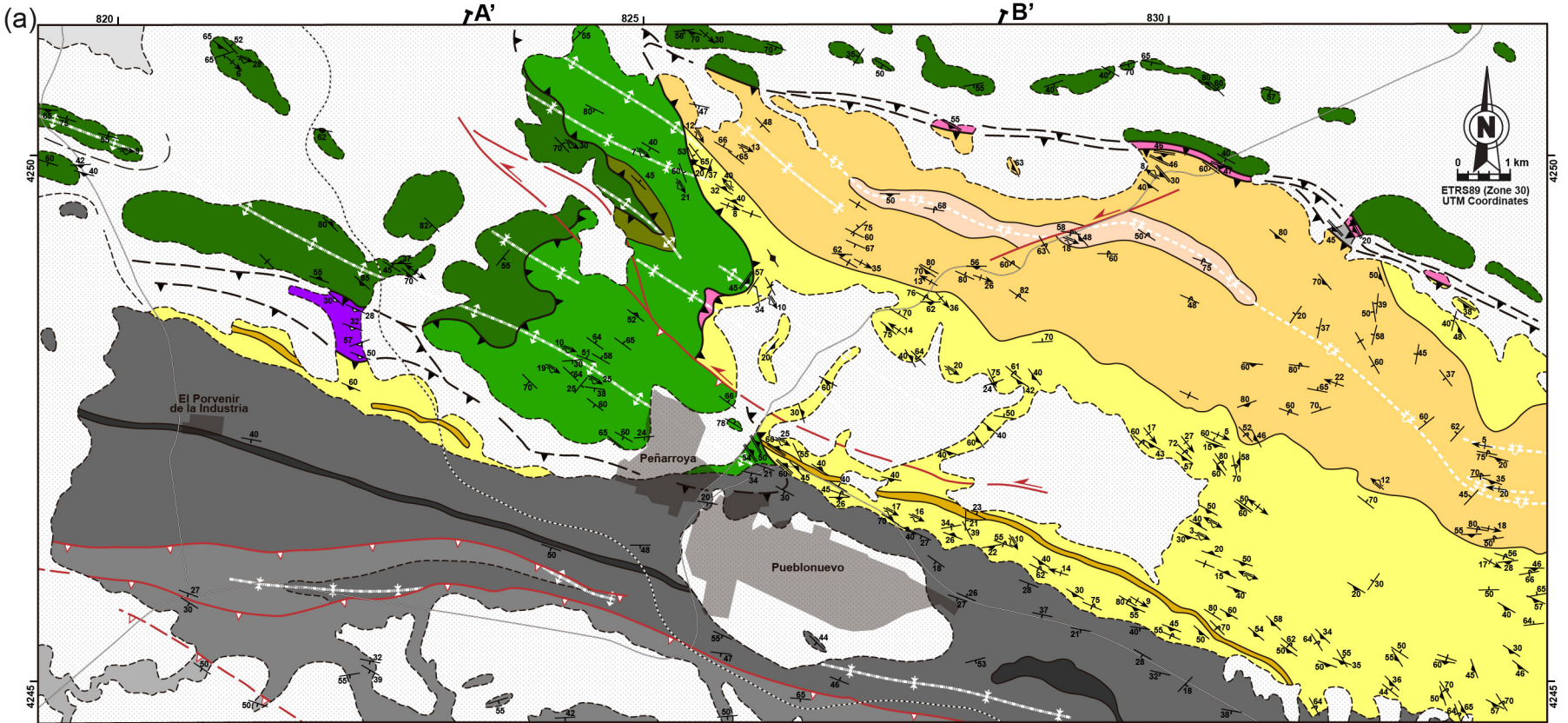
1105 **Figure 8:** Tectonic model for the Variscan obduction of the Porvenir serpentinites. (a)
1106 Devonian subduction-accretion directed to the SW. (b) Early Carboniferous out-of-
1107 sequence thrusting directed to the NE. Note that erosion is required to conclude the
1108 exhumation process. The primary geometry of the units within the suture zone are
1109 oversimplified (rather continuous and tabular-shaped) for clarity.

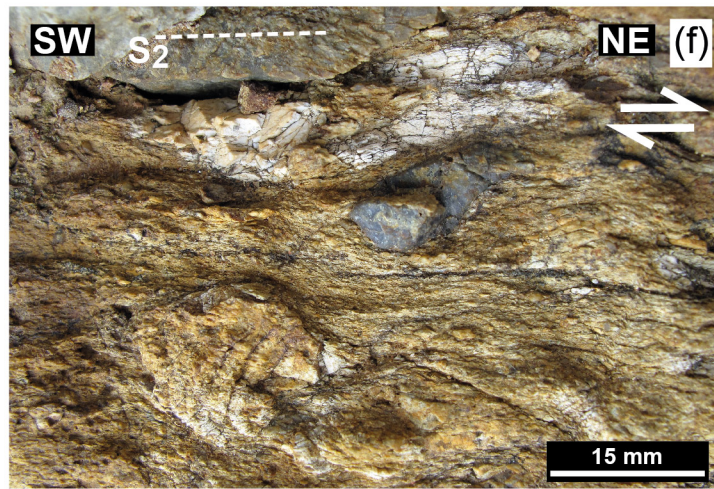
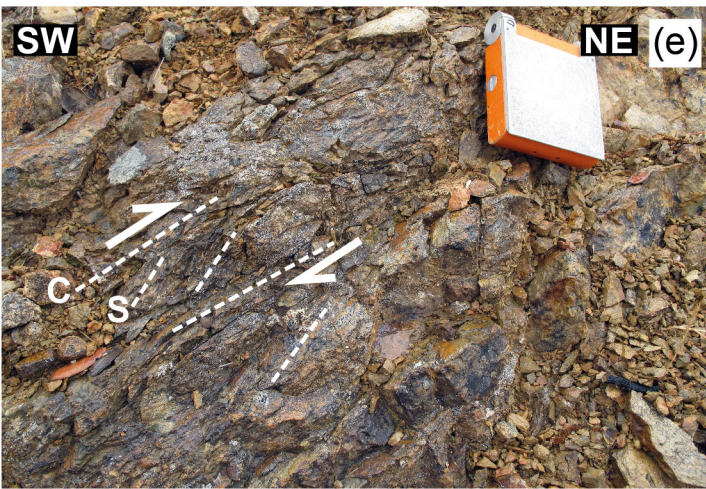
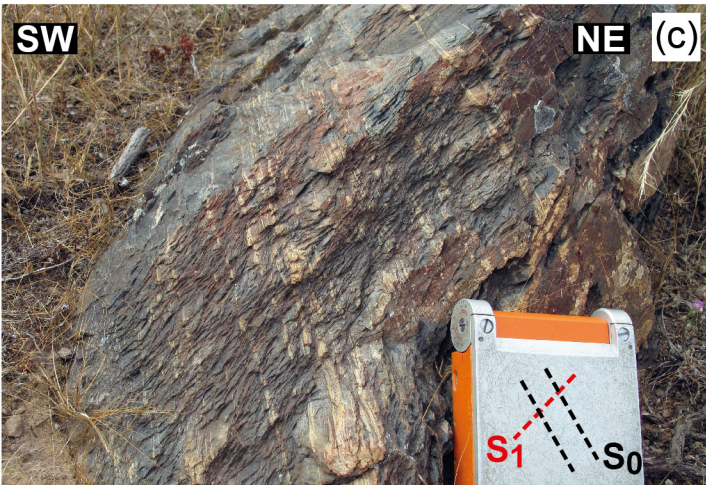
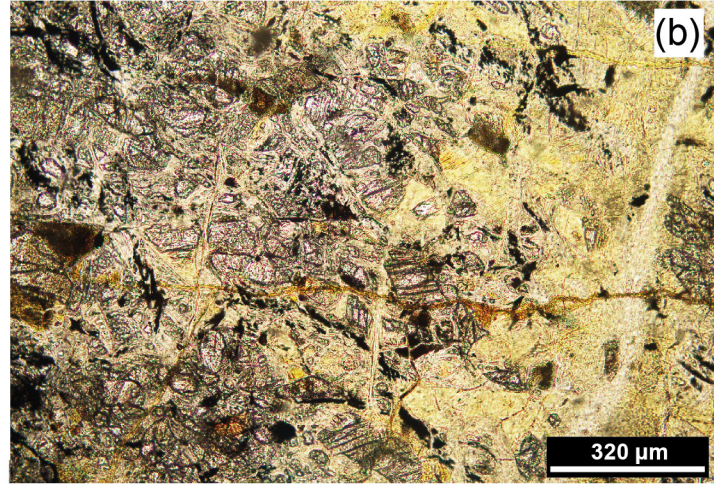
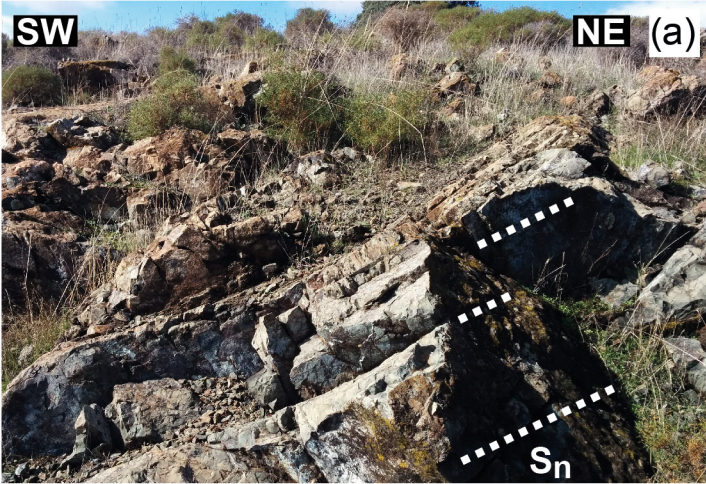
1110



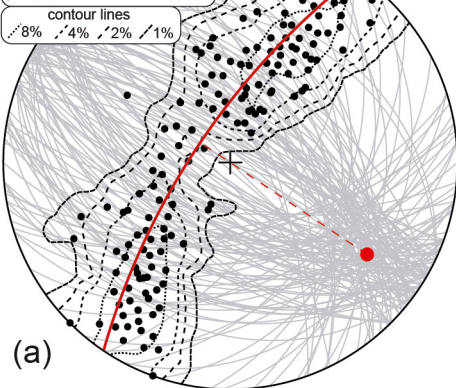






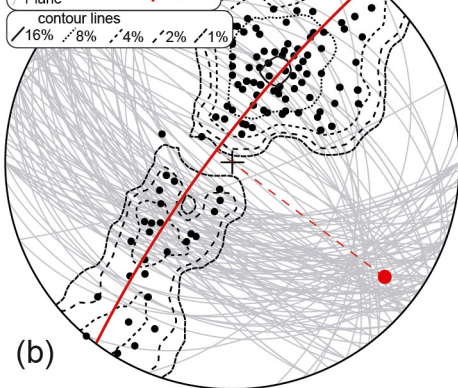


S₀ BEDDING (D₃ fold axis)
 (n=147) π AXIS (D₃) ● (18°/124°)
 ● Pole to plane
 / Plane / π -plane



(a)

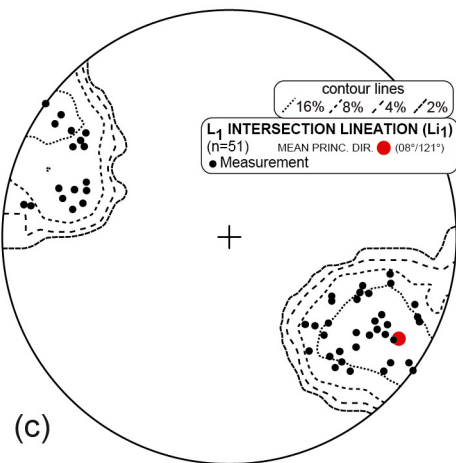
S₁ FOLIATION (D₃ fold axis)
 (n=118) π AXIS (D₃) ● (10°/127°)
 ● Pole to plane
 / Plane / π -plane



(b)

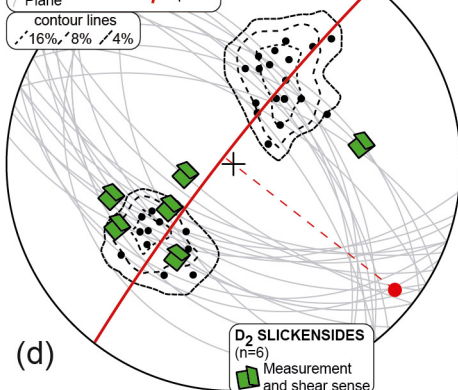
contour lines
 /16% /8% /4% /2%

L₁ INTERSECTION LINEATION (Li1)
 (n=51) MEAN PRINC. DIR. ● (08°/121°)
 ● Measurement



(c)

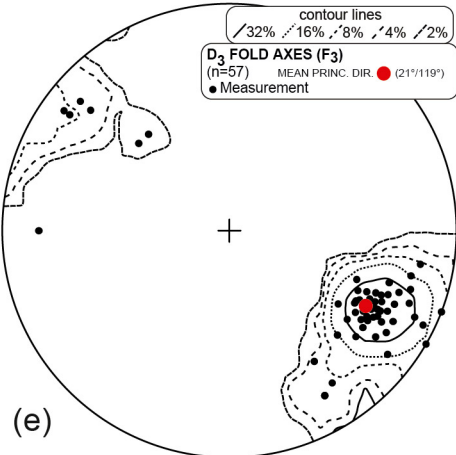
S₂ FOLIATION (D₃ fold axis)
 (n=31) π AXIS (D₃) ● (06°/128°)
 ● Pole to plane
 / Plane / π -plane



(d)

contour lines
 /32% /16% /8% /4% /2%

D₃ FOLD AXES (F₃)
 (n=57) MEAN PRINC. DIR. ● (21°/119°)
 ● Measurement



(e)

